Escola Tècnica Superior d'Enginyeries
Industrial i Aeronàutica de Terrassa
UNIVERSITAT POLITÈCNICA DE CATALUNYA

Titulació:

GRAU EN ENGINYERIA EN TECNOLOGIES INDUSTRIALS

Alumne:

MIREIA COLL CAMPRUBÍ

Títol TFG:

STUDY FOR THE NUMERICAL RESOLUTION OF CONSERVATION EQUATIONS OF MASS, MOMENTUM AND ENERGY TO BE APPLIED ON HEATING, VENTILATION AND AIR-CONDITIONING (HVAC).

Director del TFG:

ASENSI OLIVA LLENA

Co-director del TFG:

FRANCESC XAVIER TRIAS MIQUEL

Convocatòria de lliurament del TFG:

QUADRIMESTRE DE PRIMAVERA 2014-2015.

Contingut d'aquest volum:

DOCUMENT 1. - MEMÒRIA

Agraïments

Vull agrair la col·laboració de totes aquelles persones i institucions que han fet possible la realització d'aquest Treball de Final de Grau.

En primer lloc vull agrair a la Universitat Politècnica de Catalunya, i en particular a l'Escola Tècnica Superior d'Enginyeries Industrial i Aeronàutica de Terrassa, pels quatre darrers anys que m'ha proporcionat d'escola pública i de qualitat.

En segon lloc vull agrair al doctor Asensi Oliva, per tot el suport i facilitats que m'ha lliurat tant en la realització de cursos i seminaris especialitzats en la matèria, com en la direcció d'aquest treball. Sense oblidar l'ajuda del Carlos David Pérez en la col·laboració del desenvolupament d'aquest treball.

També, vull agrair doctor Francesc Xavier Trias per tota l'ajuda proporcionada, davant de tots els dubtes de la matèria que m'han anat sorgint i que sempre s'ha mostrat disposat a resoldre'ls.

I en general, també cal agrair a tot el Centre Tecnològic de Transferència de Calor per la seva dedicació i motivació en ensenyar sobre els mètodes numèrics i la dinàmica computacional de fluids.

Abstract

The study consist, as its name says, in the resolution of the Navier-Stokes equations applied to solving concrete engineering cases.

Going into more detail, this study is divided in three basic parts.

The first consist in the explanation of the involved theory that is behind the implementation of a code that solves a CFD&HT problem, as well as the numerical methods and the physics involved.

In the second part of the study, is where is entered in detail on the resolution of four concrete cases. Those four practical cases have been develop in order to learn and accomplish the knowledge needed to be able to solve cases more closer to the real engineering applications. And at the same time, to verify that the implemented codes are correct, while comparing the obtained result with the benchmark ones.

Finally, in the third part is entered in the detail of solving a concrete case of a propriety engineering application. This case consists in studying the air conditioning behaviour of a room (HVAC&R), through programing the code and analysing the obtained results.

Resumen

El trabajo consiste, tal como su nombre dice, en la resolución de las ecuaciones de Navier-Stokes aplicadas a solucionar casos concretos de ingeniería.

Entrando en más detalle, el trabajo se divide en tres partes básicas.

La primera consiste en la explicación de toda la teoría que hay detrás de la implementación de un código que solucione un problema de CFD&HT, así como los métodos numéricos y la física involucrada.

En la segunda parte del trabajo, es dónde se entra en detalle en la resolución de cuatro casos concretos. Estos cuatro casos prácticos se han realizado con el objetivo de aprender y conseguir los conocimientos necesarios para poder resolver casos más cercanos a una aplicación real de ingeniería. Y a la misma vez, para verificar que los códigos implementados son correctos, mediante la comparación de los resultados obtenidos con los de referencia.

Finalmente, en la tercera parte se entra en detalle a resolver un caso concreto de aplicación propiamente de ingeniería. Este caso consiste en estudiar la climatización de una habitación, mediante programando el código y analizando los resultados obtenidos.

Resum

El treball consisteix, tal com diu el seu nom, en la resolució de les equacions de Naveir-Stokes aplicades a solucionar casos concrets d'enginyeria.

Entrant més en detall, el treball es divideix en tres parts bàsiques.

La primer consisteix en l'explicació de tota la teoria que hi ha darrera la implementació d'un codi que solucioni un problema de CFD&HT, així com els mètodes numèrics i la física involucrada.

En la segona part del treball, és on s'entra en detall en la resolució de quatre casos concrets. Aquests quatre casos pràctics s'han realitzat amb l'objectiu d'aprendre i assolir els coneixements necessaris per poder resoldre casos més propers a una aplicació real d'enginyeria. I alhora, per verificar que els codis implementats són correctes, mitjançant la comparació dels resultats obtinguts amb els de referència.

Finalment, en la tercera part s'entra en detall a resoldre un cas concret d'aplicació pròpiament d'enginyeria. Aquest cas consisteix en estudiar la climatització d'una habitació, tot programant el codi i analitzant els resultats obtinguts.

INDEX

List of figures

List of tables

NOMENCLATURE

Table 1 - Symbols of Latin letters.

Symbol	Definition	SI units
c_p	Heat capacity	$\mathrm{J/(kgK)}$
C_{conv}	Convective coefficient stability criterion	-
C_{visc}	Viscous coefficient stability criterion	-
g	Gravity	$\mathrm{m/s^2}$
k	Thermal conductivity	$\mathrm{W/(m \cdot K)}$
p	Pressure	$\mathrm{Pa = N/m^2}$
S	Source term	$\mathrm{W/m^3}$
t	Time	s
T	Temperature	K
u	Velocity component in horizontal direction	$\mathrm{m/s}$
v	Velocity component in vertical direction	$\mathrm{m/s}$
V	Volume	$\mathrm{m^3}$
x	Axial coordinate	m
y	Normal coordinate	m

Table 2 - Symbols of Greek letters.

Symbol	Definition	SI units
α	Thermal diffusivity	$\mathrm{m^2 \cdot s}$
β	Volumetric coefficient of thermal expansion	$\mathrm{K^{-1}}$
Γ	General diffusive coefficient	1
ρ	Density	$\mathrm{kg/m^3}$
μ	Dynamic viscosity	$\mathrm{Pa \cdot s}$
ν	Kinematic viscosity	$\mathrm{m^2/s}$
ϕ	Generic variable	-
δ	Convergence error	-

Table 3 - Symbols of mathematical expressions.

Symbol	Definition
∇	Gradient
$\nabla \cdot$	Divergence
∇^2	Laplacian

Table 4 - Symbols of dimensionless groups. [1]

Symbol	Definition	Value
Re	Reynolds number	$\frac{\rho U L}{\mu}$
Pr	Prandtl number	$\frac{c_p \mu}{k}$
Pe	Peclet number	$Re \cdot Pr$
Gr	Grashof number	$\frac{\beta g L^3 \Delta T}{\nu^2}$
Ra	Rayleigh number	$Gr \cdot Pr$
Nu	Nusselt number	- Defined in section 4.4.5-
Ar	Archimedes number	$\frac{g \beta h \Delta T}{{U_o}^2}$
Fr	Froude number	$Ar^{-1/2}$

Table 5- Symbols of subscripts.

Symbol	Definition
e	Est surface
E	Est node
n	North surface
N	North node
P	Volume node
s	South surface
S	South node
w	West surface
W	West node
in	Inlet

Table 6 - Table of superscripts

Symbol	Definition
n	Time instant
p	Predictor

[1] The symbol *L* in the dimensionless groups is a generic length that will be defined according to the particular geometry of the solving case.

Table 7 - Abbreviations

Abbreviation	Definition
CDS	Central Difference Scheme
CFD	Computational Fluid Dynamics
FSM	Fractional Step Method
FVM	Finite Volume Method
NS	Navier-Stokes
QUICK	Quadratic Upstream Interpolation for Convective Kinematics
UDS	Upwind Difference Scheme
HVAC	Heating, Ventilating and Air Conditioning

1. INTRODUCTION

The study is divided in six principal sections: the introduction, the state of art, the theoretical framework, and the particular cases solved where is solved a particular case, and finally the analysis of the viability of the study development ant its conclusions and the future lines applications.

In this introduction section will be explained the previous aspects that define this study. It is divided in different sections. The aim, where are explained the objectives. The scope, where are explained those tasks that will be carried out and those that will not. The basic requirements, where are defined the aspects that have to be accomplish at the end of the study. And finally the justification, where is explained the motivation and the interests of from where this project comes.

1.1. Aim

The objective of this project consists in doing a study of the numerical resolution of conservation equations of mass, momentum and energy, applied in a specific engineering problem. Furthermore, the aim of the project is to be capable of developing a CFD&HT code. And also doing its validation and verification, and definitely understand the implicated physics.

1.2. Scope

The tasks included in this project are:

- The implementation of a two-dimensional conduction transient problem.
- The implementation of two-dimensional problem of convection and diffusion, using the convection-diffusion equation to solve it.
- The implementation of two-dimensional convection problem, using the Fractional Step Method to solve the forced and the natural convection in a cavity using the NS equations.
- The implementation of a C++ code, designed to solve a specific engineering problem, which consists in a HVAC system. This code will solve the Navier-Stokes equations. And its results will be

modified in order to accomplish the Spanish normative: "Reglamento de Instalaciones Térmicas en los Edificios".

- The solutions will be obtained from the C++ code implemented. Those solutions shall be compared with the reference numerical results with the aim of validate the code. Furthermore, the code will be verified and optimized in order to have better solution, as close as possible to reality.

The tasks non-included in this project are:

- There will not be carried out any experimental study.
- The radiation will not be considered.

1.3. Basic requirements

The basic requirements of this project are:

- At the end of the project the C++ code implemented has to be compact and optimized.
- The used geometries have to be as close as possible to reality, with the aim of having good results for the particular problem solved.

1.4. Justification

This study is justified by the strong interest in the learning and the understanding of the physics and the methods that are used to solve problems about one specific field: The heat and mass transfer and fluid mechanics, used in the industrial applications.

The study could be justified in two different aspects. First of all the interest of knowing the methods and the tools that are involved when a CFD&HT is solved, and its real application in the engineering world. And secondly the special interest in one of those applications, the HVAC&R, which is the case this study is based. The two justifications are explained by order, below.

Nowadays, the numerical methods applied to solve CFD&HT problems are very used, especially in the aeronautical and automotive field.

The numerical methods are the kernel of any simulation software. They are based on them. The correct use of a simulation software means to know when something that we have just designed is well designed or not, and it prevents us of spending a lot of time constructing prototypes that we do not know if they will give the performance that we are expecting for. Then, it means reducing wasted money and a huge optimization of the project timing.

Simulation softwares are so powerful, but, there is a problem: They have to be well used, and the user has to do a good interpretation of the results in order to understand if the results are trustable. This is why projects like this are very important: the using of powerful simulations tools without knowing well what is going on inside them (numerical methods) is a time waste.

As has been said, the existing numerical techniques can be applied in a long range of industrial and non-industrial areas.

It can be found, easily, many real applications. For example in the development of aerodynamics design applied in aeronautical and automotive areas. In the figure 1.1 it can be seen an example of a CFD analysis of a car, where the lines represents how the fluid moves around it. Another example could be the HVAC&R application, which name means: Heating, Ventilation, Air Conditioning & Refrigeration. This technique it can be very useful, for example, to design a building, or help in the design. And finally, there are some examples of CFD applications less industrial as the mentioned ones. For example, the simulation of blood that flows through veins, in the medical field investigation. Or, the simulation of a bike helmet, which design is very important in order to not lose impulse. The helmet analysis can be seen in the figure 1.2.

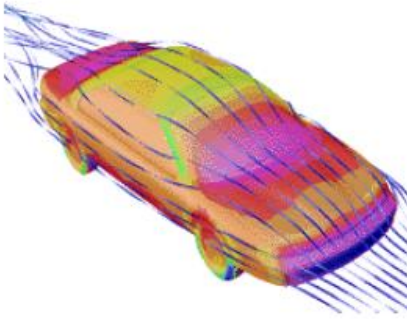

Figure 1.1 - Example of a car CFD analysis. Retrieved from D. Kuzmin, in Introduction to Computational Fluid Dynamics.

Figure 1.2 - Example of a bike helmet CFD analysis. Retrieved from: http://www.formula1-dictionary.net/cfd.html

All those showed and mentioned examples have the same thing in common: its simulation is based in the resolution of Navier-Stokes equations. Because of the inability of solve these equations by analytical methods, the way to solve them is by making numerical effective approaches.

The second aspect that justifies the study, as it has been commented in the beginning, is the application of the resolution of the NS equations in solving a real engineering problem. This particular case consists in HVAC.

The definition of the HVAC abbreviation is: "Heating, ventilating, and air-conditioning" according to Merriam-Webster [1]. So, as its name says the HVAC is the system used to operate in buildings, offices or houses in order to maintain the desired environmental conditions.

Some examples of the importance of the HVAC systems are explained next.

In the next figure 1.3, it can be seen a CFD simulation of a server room, where is very important to have a good HVAC system because this kind of rooms generate an amount of heat from the computers and machines.

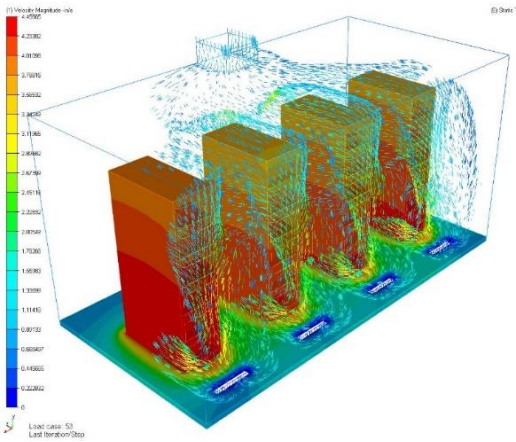

Figure 1.3 - HVAC simulation of a server room. Retrieved from: https://thevirtualengineer.wordpress.com/page/23

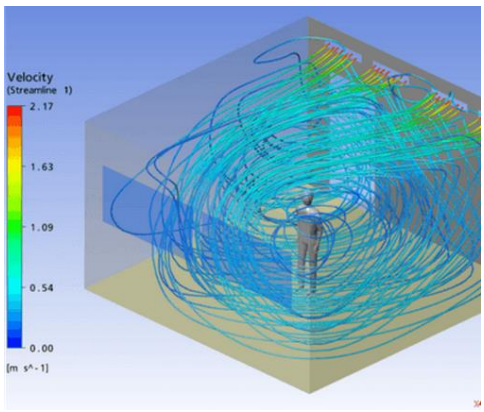

Figure 1.4 - CFD simulation of a HVAC room system. Retrieved from: www.cabraeng.com/eng/Engineering/Areas/HVAC

Another illustrative example could be a simple room where the objective is provide the thermal comfort to the people inside. In the figure 1.4 it can be seen how the velocity is distributed inside the room and around the person.

Furthermore, the air conditioning and ventilation can be applied to solve the temperature variation, the thermal loads, particle loads, and the mixed of different gases in forced or natural convection. Due to that, there are some interesting examples of its application as the optimization of heat exchangers or the fire simulations, smoke removal, evacuation and thermal loads.

In conclusion, the aim of the study is to understand how CFD&HT methods work, and be able to implement a specific case applied in HVAC&R, taking into account the importance of being able to do a good interpretation of the obtained result in order to find the correct solution.

2. STATE OF THE ART

In the antiquity, Archimedes (287-212 BC, Greece) initiated the field of static mechanics and hydrostatics. A hundred of years after that, Leonardo da Vinci (1452-1519, Italy) made contributions to the fluid mechanics by observing and describing its natural behaviour in pictures. The figure 1.5 shows two examples of his drawings.

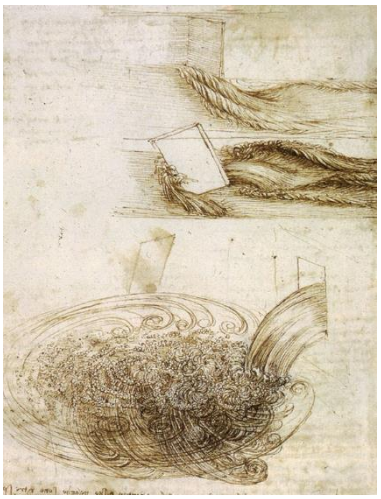

Figure 1.5 - Fluid mechanic studies by Leonardo da Vinci.
Retrieved from: http://simple.wikipedia.org/wiki/Fluid_mechanics

Years before, in the 1600's Isaac Newton (1643-1727, England) made his contributions to fluid mechanics by defining, apart from the second law, the concept of the Newtonian viscosity.

Then, in the 18th and 19th centuries was made a real change of the history of fluids, because there was a lot of work trying to describe, mathematically, their behaviour. Some of the most important contributions are commented below.

- Daniel Bernoulli (1700-1782) defined the Bernoulli principle.
- Leonard Euler (1707-1783) described the Euler equations.
- Claude-Louis Navier and Gabriel Stokes, in the early 1800's, defined independently in England and in France, respectively, the Navier-Stokes equations (named after their names) [2]. They found it by extending the Euler Equations [3]. Currently, those equations are the basis of the CFD.
- Osborne Reynolds (1842-1912, England) made some experiments in order to find the ratio between the inertial and viscous forces of a fluid, which become what it is known as Reynolds number.

In the 20th century, the theoretical works started to focus in defining the theories that describe the turbulence. Ludwig Prandtl (1875-1953) about boundary layer theory, compressible flows and the definition of the Prandtl number in that time it can be found some studies like. Geoffrey Ingram Taylor (1886-1975), who introduce the statistical theory of Taylor microscale of turbulence. Andrey Nikolayevich Kolmogorov (1903-1987) defined the Kolmogorov scales and the energy spectrum in turbulence. George Keith Batchelor (1920-2000) made some contributions in the homogeneous turbulence theory.

Furthermore, as the analytic solution of the Navier-Stokes equations does not exist, except in very exceptional situations of simple cases. As a matter of fact, to solve the real engineering problems are not analytically solved. Due to that, in the early 20th starts to born the first numerical methods capable of solving those equations numerically using super-computers. And that was when the Computational Fluid Dynamics (CFD) born.

In addition, some of the most advancing studies and research in that century where:

- In 1922 Lewis Fry Richardson (1881-1953) defined the weather prediction system by dividing the space into grid cells and finite difference approximations of the "primitive differential equations".
- In 1993 Alexander Thom (1894-1985) make the earliest numerical solution of a flow past a cylinder [4].
- In 1953, Mitutosi Kawaguti obtained a solution of a flow around a cylinder using mechanical desk calculation, and it was working for 20 hours per week for 18 months! [5].
- In the 1960's, "Los Alamos", a division of NASA start contributing with many numerical methods that are still used in this days, as vorticity-stream function methods, Particle-In-Cell (PIC), etc.
- In the 1970's a group of the Imperial College of London, under the D. Brian Spalding, developed the upwind differencing, the SIMPLE algorithm, and more useful methods.
- In 1980, Suhas V. Patankar publishes the "Numerical Heat Transfer and Fluid Flow" [6], which book has been one of the most influential one into the developing of CFD.
- In 1980's, it began to appear the commercial CFD codes, as Fluent or CFX, in order to do not have to write programme a code if you want to perform a CFD calculation. Thereby, the dependence of the CFD into the computer technology began. Because, as soon as the computers become more powerful, the time simulation of the CFD turns more available.

Currently, the CFD is recognized as an important part of the computer-aided engineering (CAE), very used in the industries to approach the modelling of a fluid flow phenomena with the possibility to solve that problem using a computer. Actually, the CFD has become indispensable to the engineering design of aerodynamics, for example for a plane or an automobile. Nevertheless, the current studies that are being developed now are focus in the optimization of those CFD codes to solve the turbulence.

3. THEORETICAL FRAMEWORK

In this section is described the theoretical framework behind the practical cases. Firstly, there is an explanation of governing equations that describe the movement of a fluid, which are the Navier-Stokes equations. Secondly, it is explained the Finite Volume Method (FVM) which is a useful methodology used in heat and mass transfer to transform the NS equations in its derivative mode to a discreet equations that could be solved numerically. Thirdly, it is explained some of the most used numerical schemes. Furthermore, the Fractional Step Method (FSM) is explained in order to describe the method used in this study to solve the NS equations. And finally, there are explained some methods of how to solve, numerically, the equations systems and the common boundary conditions used to solve the problems.

3.1. The governing equations

The general form of the Navier-stokes equations is,

$$\frac{\partial \rho}{\partial t} + \nabla \cdot (\rho \vec{u}) = 0 \tag{3.1}$$

$$\frac{\partial (\rho \vec{u})}{\partial t} + \nabla \cdot (\rho \vec{u}\vec{u}) = -\nabla p + \rho \vec{g} + \nabla \cdot \vec{\tau} \tag{3.2}$$

$$\frac{\partial (\rho (e_i + e_c))}{\partial t} + \nabla \cdot \left(\rho \vec{u}(e_i + e_c)\right) = -\nabla \cdot (\vec{u}p) - \nabla \cdot \vec{q} + \rho \vec{g}\vec{u} + \nabla(\vec{u} \cdot \vec{\tau}) \tag{3.3}$$

The first one, number 3.1 is found by the application of the mass conservation principle. The second one, number 3.2 corresponds to the momentum equation, founded by the application of the momentum conservation principle. As it is wrote in the vector form it is cannot be appreciate the three components of the velocity, but they are. And finally, the third equation number 3.3 corresponds to the application of the first and the second thermal principles in a control volume, which becomes the energy equation principle.

Nevertheless, these equations can be rewritten in the following form, firstly assuming the next considerations:

- Bidimensional model
- Laminar and incompressible flow
- Newtonian fluid
- Boussinesq hypothesis
- Negligible viscous dissipation
- Negligible compression or expansion work
- Non-participating medium in radiation

Assuming these point, the rewritten equations from 3.1 to 3.3 are:

$$\frac{\partial u}{\partial x}+\frac{\partial v}{\partial y}=0 \tag{3.4}$$

$$\rho\frac{\partial u}{\partial t}+\rho u\frac{\partial u}{\partial x}+\rho v\frac{\partial u}{\partial y}=-\frac{\partial p}{\partial x}+\mu\left(\frac{\partial^2 u}{\partial x^2}+\frac{\partial^2 u}{\partial y^2}\right) \tag{3.5}$$

$$\rho\frac{\partial v}{\partial t}+\rho u\frac{\partial v}{\partial x}+\rho v\frac{\partial v}{\partial y}=-\frac{\partial p}{\partial y}+\mu\left(\frac{\partial^2 v}{\partial x^2}+\frac{\partial^2 v}{\partial y^2}\right)+\rho g\beta(T-T_\infty) \tag{3.6}$$

$$\rho\frac{\partial T}{\partial t}+\rho u\frac{\partial T}{\partial x}+\rho v\frac{\partial T}{\partial y}=\frac{k}{c_p}\left(\frac{\partial^2 T}{\partial x^2}+\frac{\partial^2 T}{\partial y^2}\right)+\frac{\Phi}{c_p} \tag{3.7}$$

The first one, number 3.4, is known as the continuity equation. The equations 3.5 and 3.6 are the momentum in horizontal and vertical direction, respectively. And the last one, number 3.7, is the energy equation. Those equations describe how the velocity, density, pressure and temperature of a moving fluid are related.

All the Navier-Stokes equations can be summarized in the convection-diffusion equation:

$$\frac{\partial(\rho\phi)}{\partial t}+\nabla(\rho\vec{u}\phi)=\nabla(\Gamma\nabla\phi)+S \tag{3.8}$$

This equation shows that the accumulative term (also known as transient term) plus the net convective flow has to be equal to the net diffusion plus the net generation of ϕ, per unit of volume.

In the next table, 3.1, it is summarized the general values of the convection-diffusion equation that has to be replaced in each case in order to reproduce the governing equations (as in equations from 3.4 to 3.7).

Table 3.1 – General parameters to replace in convection-diffusion equation in order to reproduce the governing equations.

	ϕ	Γ	S
Mass conservation equation	1	0	0
Momentum equation (in x direction)	u	μ	$-\frac{\partial p}{\partial x}$
Momentum equation (in y direction)	v	μ	$\frac{\partial p}{\partial x}+\rho g\beta(T-T_\infty)$
Energy conservation equation (with constant c_p)	T	λ/c_p	Φ/c_p

3.2. Finite Volume Method

To obtain an approximate numerical solution, it is needed a discretization method in order to transform the differential equations in a system of algebraic equations, that can be solved on a computer. There are some different methods of approximating the differential equations by a system of algebraic. The most commons are the finite difference (FC), finite element (FE) and the finite volume (FV). Nevertheless in this study it was used the last one and in this section it will be explained.

The finite volume method (FVM) divides the domain into a finite number of contiguous control volumes. The figure 3.1 describes the control volume formulation in two dimensions.

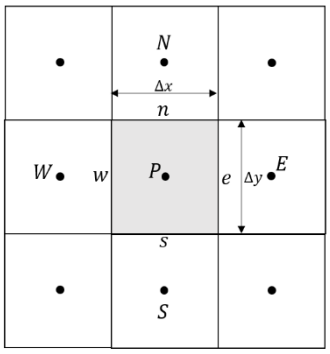

Figure 3.1 - Two-dimensional control volume formulation.

In order to explain the FVM the convection-diffusion equation will be used. Rewriting the equation:

$$\frac{\partial(\rho\phi)}{\partial t} + \nabla(\rho\vec{u}\phi) = \nabla(\Gamma\nabla\phi) + S \tag{3.8}$$

To discretize this equation following the FMS method, it is needed to integer all the equation into the its volume:

$$\int \left(\frac{\partial(\rho\phi)}{\partial t} + \nabla(\rho\vec{u}\phi) = \nabla(\Gamma\nabla\phi) + S \right) \partial\Omega \tag{3.9}$$

With the aim to transform the volume integration into a surface integration it is applied the Gauss Theorem[2], and the results is shown term by term in the following explanation.

- The diffusion term:

$$\int_\Omega \nabla(\Gamma\nabla\phi)\,\partial\Omega = \int_{\partial\Omega} \Gamma(\nabla\phi)\cdot\vec{n}\,\partial S = \Gamma\int_e \frac{\partial u}{\partial x}\,\partial y - \Gamma\int_w \frac{\partial u}{\partial x}\,\partial y + \\ + \Gamma\int_n \frac{\partial v}{\partial y}\,\partial x - \Gamma\int_s \frac{\partial v}{\partial y}\,\partial x \tag{3.10}$$

[2] The Gauss Theorem transforms a volume integration into a surface integration. The mathematic expression is: $\int_\Omega \nabla\cdot\vec{a}\ \partial\Omega = \int_{\partial\Omega} \vec{a}\cdot\vec{n}\,\partial S$. Where Ω is the volume, $\vec{a}$ is a generic variable and $\vec{n}$ the normal direction of that generic variable.

- The convective term:

$$\rho \int_{\Omega} \nabla(\vec{u}\phi)\, \partial\Omega = \int_{\partial\Omega} \rho(\vec{u}\cdot\phi)\cdot\vec{n}\, \partial S = \rho \int_{e} u\phi\, \partial y - \\ -\rho \int_{w} u\phi\, \partial y + \rho \int_{n} v\phi\, \partial x - \rho \int_{s} v\phi\, \partial x \qquad (3.11)$$

For the transient and the source term is no needed to apply the Gauss Theorem, because its integration is directly. Moreover, to evaluate the remaining integrals of the equations 3.11 and 3.12, in the next section 3.3 will be explained.

3.3. Numerical schemes

To calculate the convective and diffusive fluxes, it is needed to evaluate the value of ϕ[3] and its gradient normal to the cell face at each control volume of the domain. This evaluation has to be expressed in terms of the nodal values by interpolation, due to the value of ϕ is known at the cell centre.

There are numerous available possibilities. Some of the most known and used ones are explained next.

- Central Difference Scheme (CDS)
  It is a second order scheme. The value of ϕ is calculated using a linear interpolation between the two neighbouring values. It becomes an arithmetic mean if its assumed a regular mesh where Δx is constant.

$$\phi_e = \frac{1}{2}(\phi_E + \phi_P) \qquad (3.12)$$

- Upwind Difference Scheme (UDS)
  It is a first order scheme and the value of ϕ at the cell face depends of the direction of the mass flow. Has no convergence problems.

$$\phi_e = \phi_E \quad if \quad \dot{m}_e > 0 \qquad (3.13a)$$
$$\phi_e = \phi_P \quad if \quad \dot{m}_e < 0 \qquad (3.13b)$$

- Hybrid Difference Scheme (HDS)
  This scheme is a combination of CDS and UDS. It uses CDS for low velocities and HDS for high velocities.

[3] ϕ is a general variable. It could represent the temperature or the velocities. Please refer to section X.XX where it is explained the convection-diffusion equation to see that more clearly.

- Exponential Difference Scheme (EDS)
  It is a second order scheme and the value of ϕ at the cell face comes from the exact solution of the convection-diffusion equation in one-dimensional, considering null source term and steady problem.

$$\phi_e = \phi_P \cdot e^{\frac{\rho u_{xe} d_{Pe}}{\Gamma_e}} \qquad (3.14)$$

- QUICK Scheme
  This scheme consist in a quadratic interpolation in function of the direction of mass flow. Also is a combination of UDS and a high order interpolation, because depends of the direction of the mass flow.

$$\phi_e = \frac{\phi_E + \phi_P}{2} - \frac{\phi_W - 2\phi_P + \phi_E}{8} \quad if\ \dot{m}_e > 0 \qquad (3.15a)$$

$$\phi_e = \frac{\phi_E + \phi_P}{2} - \frac{\phi_P - 2\phi_E + \phi_{EE}}{8} \quad if\ \dot{m}_e < 0 \qquad (3.15b)$$

To see the formulation of higher-order schemes please refer to Ferziger and Peric [7] or Patankar [6].

3.4. Fractional Step Method

The Fractional Step Method (FSM) is the most common technique for solving the incompressible Navier-Stokes equations, introduced in the 1960's for Harlow and Welch [8], and Chorin [9].

The FSM uses a projection method in order to find the velocity (predictor velocity) without considering the pressure gradient. And afterwards, to its correction considering that pressure gradient.

3.4.1. Helmholtz-Hodge theorem

The Helmholtz-Hodge theorem plays an important role in the decomposition of the incompressible Navier-Stokes equations in the FSM, and the definition of the pressure role.

The theorem says:

> *A given vector field ω, defined in a bounded domain Ω with a smooth boundary $\delta\Omega$, is uniquely discomposed in a pure gradient field and a divergence-free vector parallel to $\delta\Omega$.*

$$\omega = a + \nabla\varphi \tag{3.16}$$

Where,

$$\nabla \cdot a = 0 \qquad a \in \Omega \tag{3.17a}$$
$$a \cdot n = 0 \qquad a \in \partial\Omega \tag{3.17b}$$

Directly citation from [10].

If this decomposition is applied into the Navier-Stokes equations it is obtain a unique separation as can be seen in the following expression in equation 3.18.

$$\Delta p = \nabla \cdot \left(-(u \cdot \nabla)\, u + \frac{1}{Re} \Delta u \right) \tag{3.18}$$

Nevertheless, to visually understand this unique decomposition, please refer to the figure 3.2 where it is shown its algebraic representation.

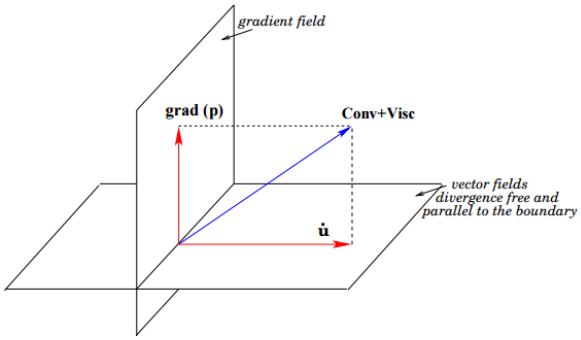

Figure 3.2 - Vector field decomposition.
Retrieved from: Introduction to the Fractional Step Method [10]

3.4.2. Implementation of the FSM

Re writing the Navier-Stokes equations (equations from 3.1 to 3.4 in the section 3.1) in the differential and vector form, we obtained:

$$\nabla \cdot \vec{u} = 0 \tag{3.19}$$

$$\rho \frac{\partial \vec{u}}{\partial t} + (\rho \vec{u} \nabla)\vec{u} = \mu_o \nabla^2 \vec{u} - \nabla \vec{p} \tag{3.20}$$

Putting together the convective and the diffusive term:

$$R(\vec{u}) = -(\rho \vec{u} \nabla)\vec{u} + \mu_o \nabla^2 \vec{u} \tag{3.21}$$

The momentum equation (3.20) can be written as next:

$$\rho \frac{\partial \vec{u}}{\partial t} += R(\vec{u}) - \nabla \vec{p} \tag{3.22}$$

In order to discretize the NS equation as is written in the equation 3.22, it was been used a central difference scheme (CDS) for the time derivative term[4]. A full explicit second-order Adams-Bashforth scheme for $R(u)$[5]. And finally, a first-order backward Euler scheme for the discretization of the pressure-gradient term. Therefore, the semi-discretized Navier-Stokes equations was found:

$$\rho \frac{u^{n+1} - u^n}{\Delta t} V_P = \frac{3}{2} R(u^n) - \frac{1}{2} R(u^{n-1}) - \nabla \cdot p^{n+1} \tag{3.23}$$

$$\nabla \cdot u^{n+1} = 0 \tag{3.24}$$

To solve the velocity-pressure, it is used the velocity projection from the Helmholtz-Hodge theorem, which explains the methodology of vector decomposition. (See section 3.4.1 of Helmholtz-Hodge theorem).

From this theorem what we get is the next decomposition:

$$u^p = u^{n+1} - \nabla \tilde{p} \tag{3.25}$$

Joining the 3.23 and 3.25 equations, it is obtained the next expression for the predictor velocity:

$$u^p = u^n + \frac{\Delta t}{\rho V_P} \left(\frac{3}{2} R(u^n) - \frac{1}{2} R(u^{n-1}) \right) \tag{3.26}$$

And then, in order to solve the pressures, the Poisson equation needs to be solved:

$$\Delta \tilde{p} = \nabla \cdot u^p \tag{3.27}$$

Once the pressures has been solved, we obtain the correction velocity by:

$$u^{n+1} = u^p - \nabla \tilde{p} \tag{3.28}$$

[4] The CDS scheme used is the following one: $\left.\frac{\partial u}{\partial t}\right|^{n+1/2} \approx \frac{u^{n+1} - u^n}{\Delta t}$

[5] The Adams-Bashforth scheme makes the following interpolation between the current and the previous instant: $R\left(u^{n+\frac{1}{2}}\right) \approx \frac{3}{2} R(u^n) - \frac{1}{2} R(u^{n-1})$.

Algorithm:

1. Evaluate $R(u^n)$ as it is defined in the equation 3.23. The term that includes the convective and the diffusive term is evaluated as a function of the velocity field at the previous instant (u^n).
2. Find the predictor velocity: $u^p = u^n + \frac{\Delta t}{\rho}\left[\frac{3}{2}R(u^n) - \frac{1}{2}R(u^{n-1})\right]$. Once the $R(u^n)$ has been calculated, the predictor velocity is calculated as a function of the velocity at the previous instant (u^n).
3. Solve the Poisson equation: $\Delta p^{n+1} = \frac{\rho}{\Delta t}\nabla \cdot u^p$. Using the predictor velocity the pressures are solved.
4. Obtain the new velocity field: $u^{n+1} = u^p - \frac{\Delta t}{\rho}\nabla p^{n+1}$. Once the pressures are solved, we used them to find the correct velocity.

3.4.3. The checkerboard problem

If a 1D discretization is made on the third step of the previously Fractional Step Method, a problem occurs.

$$u^{n+1} = u^p - \frac{\Delta t}{\rho}\left(\frac{p_E^{n+1} - p_W^{n+1}}{2\Delta x}\right) \tag{3.29}$$

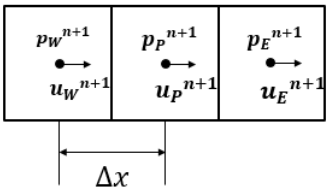

Figure 3.3 - 1D FSM discretization.

The discretization is explained in the figure 3.3. In the figure it can be seen how the approximation of pressure gradient of the node P is independent of the pressure of the same node (It can be notice of that because the p_P does not appear in the pressure gradient terms for the control volume equations at P). That means that it would be possible to obtain converged velocity fields for unphysical pressure phenomena distributions.

In order to solving this problem there are two available options that have been developed to solve this problem. The staggered meshes and the collocated meshes. The staggered mesh solves the checkerboard problem by having the velocity at the faces. And the collocated meshes have the velocity at the main centre of the control volume.

The method to solve the checkerboard problem by using staggered meshes is detailed below in the section 3.4.4.

3.4.4. Staggered mesh

In the case of using staggered mesh, the nodes of velocity are situated in the faces of the control volume. To do so, it is needed to have a different mesh for the velocities.

Following this method, if it is used a uniform mesh, it would be needed 3 different meshes: one for the horizontal component of the velocity, another one for the vertical component of the velocity, and finally another one for the pressure. In the figure 3.4, it can be seen more clearly.

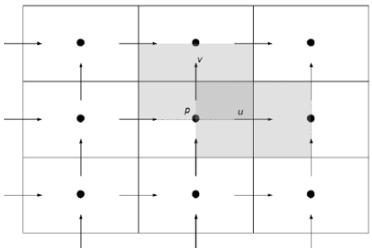

Figure 3.4 - Staggered mesh formulation.

Following the scheme of the figure 3.4 the pressures will be solved in the centred mesh, but each velocity component will be solved in its staggered mesh.

3.4.5. Determination of the time step Δt

When an explicit temporal scheme is used can appear some stability problem, which will be solved by using a condition for convergence.

To solve this problem, in our case, the time step must be founded by the CFL condition[6] [11], which is given by:

$$\Delta t \left(\frac{|u_i|}{\Delta x_i}\right)_{max} \leq C_{conv} \tag{3.30}$$

$$\Delta t \left(\frac{\nu}{\Delta {x_i}^2}\right)_{max} \leq C_{visc} \tag{3.31}$$

Where the bounding values C_{conv} and C_{visc} are 0.35 and 0.20 respectfully, values recommended by [12].

[6] The CFL condition named in their authors surname could be found in the paper Courant, Friedrichs and Lewy [11].

3.4.6. Global FSM Algorithm

In this section it is explained the global algorithm that is needed to follow in case of solving a problem by using the FSM.

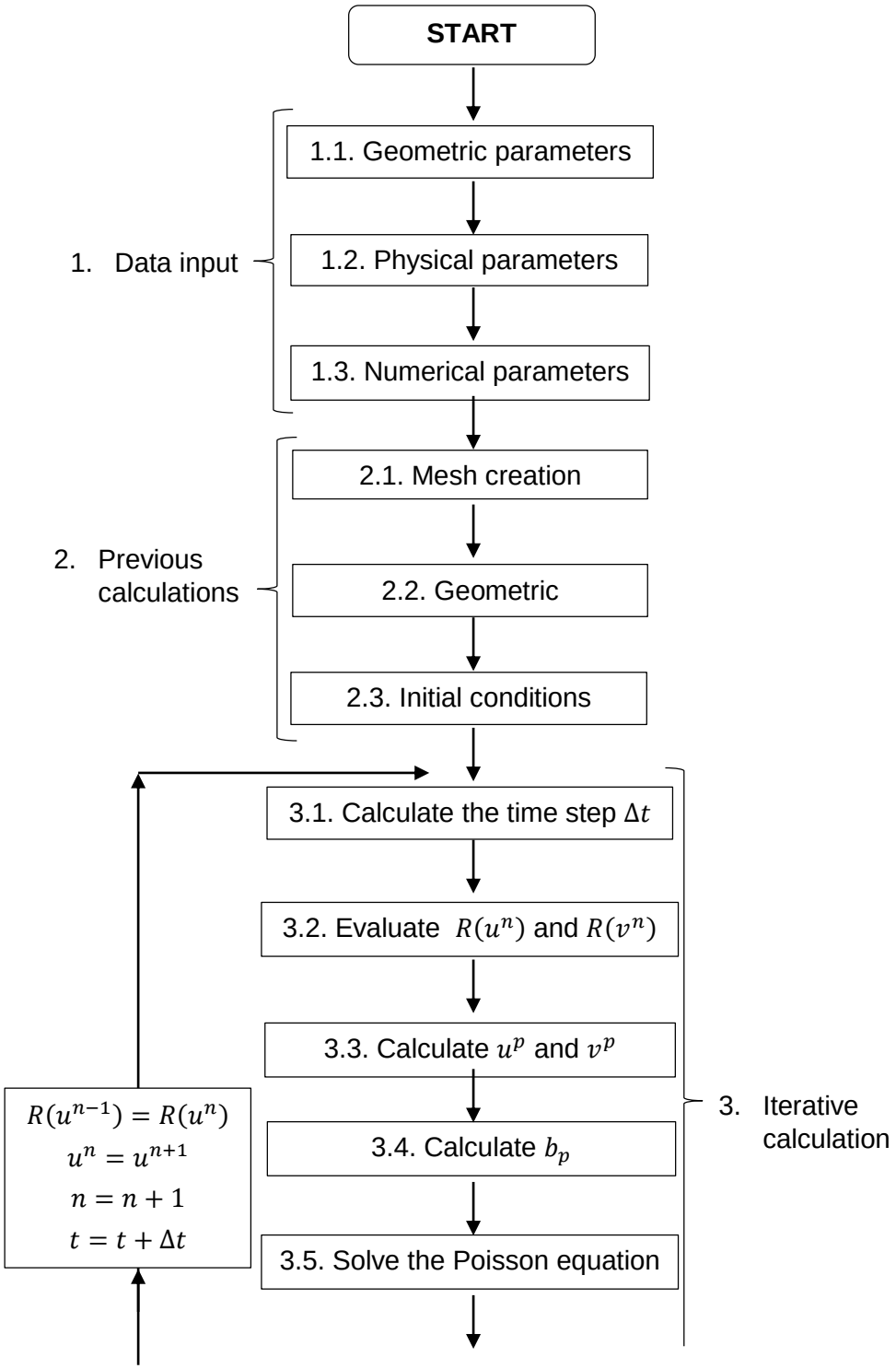

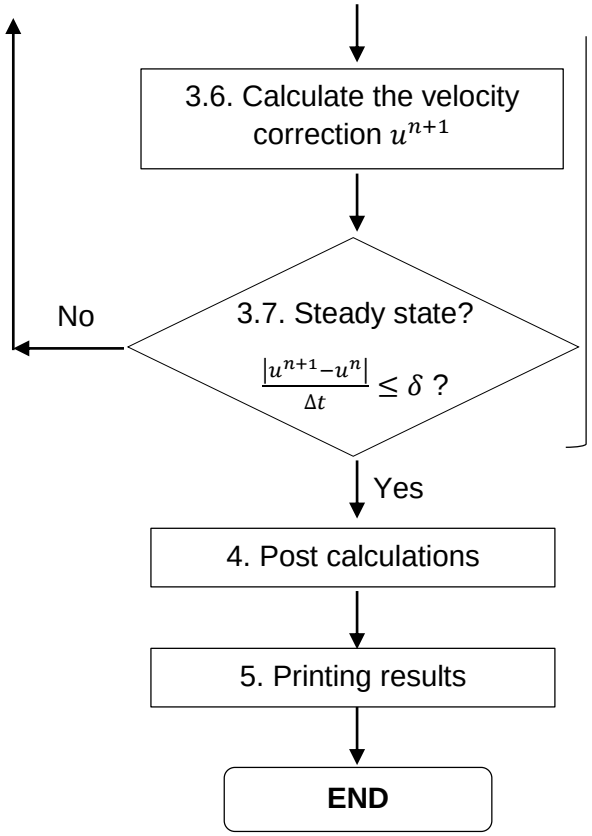

Explanation in more detail of every step of the algorithm:

1. Data input
   1.1. Geometric parameters. In this section are defined all the geometry that define the problem.

   1.2. Physical parameters. All the known and needed physics parameters are defined in this section, as the viscosity, the density, etc.

   1.3. Numerical parameters. All the known data parameters that involve the numerical resolution of the problem are defined in this section. This parameters could be the δ (the time-step error), the δ_{solver} (The maxim error of the solver if this one non-direct), etc.

2. Previous calculations
   2.1. Mesh creation. In this section the mesh is created.

2.2. Geometric coefficients. Calculation of the discretization coefficients a_p, a_E, a_W, a_N and a_S. It is only needed to run them once because they only depends on the problem mesh and geometry.

2.3. Initial conditions. Definition of the initial velocity field on the boundaries and the map pressures.

3. Iterative calculation. In this section is where the FSM as it has been explained before it is solved.
   3.1. Calculate the time step Δt, following the CFL condition.

   3.2. Evaluate $R(u^n)$ and $R(v^n)$,

   3.3. Calculate u^p and v^p.

   3.4. Calculate b_p. The geometric coefficient b_p has to be calculated at each time because it depends on the current predictor velocity.

   3.5. Solve the Poisson equation, through one of the explained solvers, like the Gauss-Seidel.

   3.6. Calculate the velocity correction u^{n+1}.

   3.7. Steady state? Check by the expression: $\frac{|u^{n+1}-u^n|}{\Delta t} \leq \delta$ if the simulation has arrived to the steady state. If it has arrived, we can go to the next step (4). But if not, it is needed to go back into the iterative mode beginning to recalculate the new time step and transfer the actual results to the orders for the post calculation.

4. Post calculations. When all the program has been ran, we just need to calculate the final parameters, like the Nusset number, etc.

5. Printing results. Finally we print the final results of the simulation. We do this at the end of the simulation in order to not waste time-calculation printing non-ultimate results.

3.5. Solvers

The equations system to be solved is the type defined in the next equation:

$$Ax = b \tag{3.32}$$

Which, written in matrix form is:

$$\begin{pmatrix} a_{11} & a_{12} & a_{13} & \cdots & \cdots & a_{1,n} \\ a_{21} & a_{22} & a_{23} & \cdots & \cdots & a_{2,n} \\ & a_{32} & a_{33} & & & \\ \vdots & \ddots & & \ddots & & \vdots \\ & & a_{n-1,n-2} & a_{n-1,n-1} & a_{n-1,n} & \\ a_{n,1} & \cdots & \cdots & a_{n,n-1} & a_{n,n} & \end{pmatrix} \begin{pmatrix} x_1 \\ x_1 \\ \vdots \\ x_n \end{pmatrix} = \begin{pmatrix} b_1 \\ b_1 \\ \vdots \\ b_n \end{pmatrix}$$

The coefficients of A and b are all know. What is it wanted to know are the values of the x matrix.

At first, it could be think that a good way to solve this equations system is directly making $x = A^{-1}b$. But, in practice that way is completely unworkable because make the inverted matrix of A requires a calculation which complicates more the problem. Due to invert the matrix A is not a good method, alternative resolution tools appear, the *solvers*.

There are two types of solvers, the direct and the iterative. The direct ones are those that while the entire matrix is solved the solution is reached. The iterative solvers, however, have to make as many interactions until an acceptable error (δ) is reached. The next equation number 3.33 shows how to check the iterative method convergence.

$$\|Ax - b\| < \delta \tag{3.33}$$

Below are explained two different types of solvers.

3.5.1. Gauss-Seidel

The Gauss-Seidel algorithm is an iterative method that solves the values of x point by point in the following manner in the equation 3.34, for each $i = 1,2,\dots n$.

$$x_i^{k+1} = \frac{1}{a_{ij}} \left(-\sum_{j<i} a_{ij}\, x_j^{k+1} - \sum_{j>i} a_{ij}\, x_j^{k} + b_i \right) \tag{3.34}$$

The new values of x_i^{k+1} are used as soon as they are known. For example, first it is computed the value of x_1^{k+1}, and once this is computed it is used in the second equation to calculate the new x_2^{k+1}, and so on.

As it is an iterative method when the x_i^{k+1} values are fond for all the domain values of i it is needed to check (for each value of i from 1 to n) if the method has converged, with the next expression.

$$\left\|x_i^{k+1} - x_i^k\right\| < \delta \tag{3.35}$$

3.5.2. TDMA

The TDMA method (its acronym of Tridiagonal Matrix Algorithm), it is a direct solver that it is a simplification of the Gauss-Seidel method.

The tridiagonal system of equations may be written as:

$$a_i x_i + b_i x_{i-1} + c_i x_{i+1} = d_i \tag{3.36}$$

Written in the matrix form,

$$\begin{bmatrix} a_1 & c_1 & & & & 0 \\ b_2 & a_2 & c_2 & & & \\ & b_3 & a_3 & c_3 & & \\ & & \ddots & \ddots & \ddots & \\ & & & b_{n-1} & a_{n-1} & c_{n-1} \\ 0 & & & & b_n & a_n \end{bmatrix} \begin{bmatrix} x_1 \\ x_2 \\ \vdots \\ x_{n-1} \\ x_n \end{bmatrix} = \begin{bmatrix} d_1 \\ d_2 \\ \vdots \\ d_{n-1} \\ d_n \end{bmatrix} \tag{3.37}$$

The method consists in directly solve the written matrix:

$$P_i = \frac{c_i}{a_i - b_i \cdot P_{i-1}} \tag{3.38a}$$

$$R_i = \frac{d_i + b_i \cdot R_{i-1}}{a_i - b_i \cdot P_{i-1}} \tag{3.38b}$$

And finally the concurrency formulae to find the direct solution for each x_i is,

$$x_i = P_i \cdot x_{i+1} + R_i \tag{3.39}$$

The way to solve is, first, calculate the values of P_i and R_i for each node in ascendant. Notice that for the first node $i = 1$: $P_1 = \frac{c_1}{a_1}$ and $R_1 = \frac{d_1}{a_1}$. Then, in order to find the x_i values, it is needed to set the $x_n = R_n$, and with the equation 3.39 find the rest of the values from $i = n - 1$ to $i = 1$ (descending order).

The disadvantage that the TDMA method has, is that it is only directly for tridiagonal matrix, as it would be if the problem is in one dimension. If the is a two or three dimension problem, some modifications has to be applied.

In the formulation for a two dimension problem, a part of the one dimensional neighbour coefficients, it appears the north and south neighbour coefficients. Therefore, the system of equations may be written as:

$$a_{ij}x_{ij} + b_{ij}x_{i-1,j} + c_{ij}x_{i+1,j} + e_{ij}x_{i,j-1} + f_{ij}x_{i,j+1} = d_i \qquad (3.40)$$

In order to transform the equation 3.40 into a system of equations as the first one (equation 3.36), the coefficients that are not wanted are included in the independent term, as:

$$d_i{}' = d_i - e_{ij}x_{i,j-1} + f_{ij}x_{i,j+1} \qquad (3.41)$$

Therefore, the earlier concurrency method explained is the same with the only difference that now the independent term is $d_i{}'$ and it is calculated as the equation 3.41. The method becomes to being iterative, because in each x_{ij} calculation there are the values of $x_{i,j+1}$ supposed from the last iteration. To check if the method has converged it can be used the same methodology as in the Gauss-Seidel (please refer to equation 3.35), and it has to be done for all the nodes of the domain.

3.6. Boundary conditions

When it is wanted to solve a simply conduction case in one dimension, it is needed to know the boundary-grid point temperatures, in order to be able to solve the rest of temperatures of the inside of the material. In other words, the boundary conditions are, practically, the most important part of a problem because is what it is needed in order to solve the problem.

There are different types of boundary conditions. The most commons are:

- Dirichlet Boundary condition (DBC). The boundary condition in any heat transfer simulation are expressed in terms of the ϕ value at the boundary, because ϕ is known.

$$\phi = ct \tag{3.42}$$

  In terms of solving the equation system, the additional equation given by using this BC is:

$$a_P = 1 \quad ; \quad b_P = ct \quad ; \quad a_i = 0 \tag{3.43}$$

  Where $i = E, W, N, S$ [7], and ct is the value of ϕ known at the boundary.

- Neumann Boundary condition (NBC). The boundary conditions is set by the ϕ gradient normal to the boundary surface. An important and quite common special case of NBC is when the boundary flux $ct = 0$. That typical case can be found in the isolated surfaces.

$$\frac{\partial \phi}{\partial n} = ct \tag{3.44}$$

  Its implementation intended to solve the equation system will be:

$$a_P = 1 \quad ; \quad b_P = 0 \quad ; \quad a_i = 0 \quad ; \quad a_{j \neq i} = 1 \tag{3.45}$$

  Where $i = E, W, N, S$ [8], and j the neighbour value of the n direction.

[7],[7] : Considering the two dimensional discretization.

- Robin Boundary Condition (CBC). The boundary condition is set by specifying the heat flux in terms of an explicit heat flux (with its convective heat transfer coefficient and the reference ϕ known value). If we are solving, for example, the temperatures, the additional equation given by this BC is:

$$-\frac{\partial T}{\partial n} = k(T_o - T) \tag{3.46}$$

Where the values of T_o is the reference known temperature.

4. PARTICULAR CASES SOLVED

Based in the theory which has been defined in earlier words, in this section are explained and solved some particular cases, particularly four problems.

The aim of this section is getting familiar with the numerical resolution algorithms, testing and validating the resolution of some particular cases that have been completely studied. The final objective will be the solving of the Navier-Stokes equations.

The first problem consists in solving a conduction problem, in two dimensions using different materials. Subsequently, the next step would be solving the convection phenomena using the convection-diffusion equation (3.8 equation). Finally, the last two problems consists in solving the Navier-Stokes equations by using the Fractional Step method, one for forced convection and the other one for natural convection.

4.1. A two-dimensional transient conduction problem

This problem consists in a very long rod composed of four different materials (M1, M2, M3 and M4), as it can be seen in the figure 4.1, below. As the draw is not a scale in the table 4.1 the coordinates of the points p_1, p_2 and p_3 are given. The properties of each one of the four materials are given in the 4.2 table, and boundary conditions can be found in the table 4.3. Furthermore, the initial temperature field is known, and is $T = 8.00\ °C$.

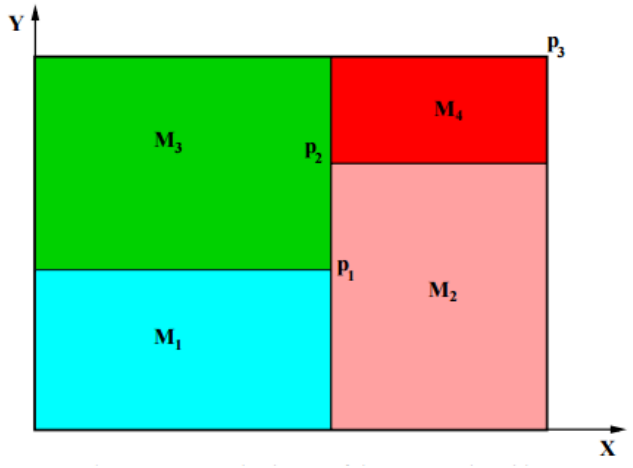

Figure 4.1 - Schema of the two-dimensional transient conduction problem. Recovered image from CTTC courses notes [https://www.cttc.upc.edu/].

Table 4.1 - Transient conduction problem coordinates.

	$x\ [m]$	$y\ [m]$
p_1	0.50	0.40
p_2	0.50	0.70
p_3	1.10	0.80

Table 4.2 - Physical properties of transient conduction problem.

	ρ [kg/m^3]	c_p [J/kg·K]	k [W/m·K]
M_1	1500.00	750.00	170.00
M_2	1600.00	770.00	140.00
M_3	1900.00	810.00	200.00
M_4	2500.00	930.00	140.00

Table 4.3 - Boundary conditions of transient conduction problem.

Cavity wall	Boundary condition
Bottom	Isotherm at $T = 23.00\ °C$
Top	Uniform $Q_{flow} = 60.00\ W/m$ length
Left	In contact with a fluid at $T_g = 33.00\ °C$ and a heat transfer coefficient of $9.00 W/m^2 K$
Right	Uniform temperature $T = 8.00 + 0.005 \cdot t\ °C$ (Where t is the time in seconds)

4.1.1. Mesh

As there are four different materials, the mesh was adapted to that. The x axe was divided in two different mesh formulation. The y axe was defined in two different mesh formulation, as the different material combinations there are. Due to, the rod was divided in six different uniform meshes.

4.1.2. Mathematical formulation of the problem

This problem consists in solving the energy equation, earlier defined in the section 3.1, and rewritten in the following equation:

$$\rho \frac{\partial T}{\partial t} + \rho u \frac{\partial T}{\partial x} + \rho v \frac{\partial T}{\partial y} = \frac{k}{c_p}\left(\frac{\partial^2 T}{\partial x^2} + \frac{\partial^2 T}{\partial y^2}\right) + \frac{\Phi}{c_p} \qquad (4.1)$$

From that equation it can be identified four different terms:

- The transient term: $\rho \frac{\partial T}{\partial t}$
- The convective term: $\rho u \frac{\partial T}{\partial x} + \rho v \frac{\partial T}{\partial y}$. Where the temperature interacts with the fluid velocities.
- The diffusion term: $\frac{k}{c_p}\left(\frac{\partial^2 T}{\partial x^2} + \frac{\partial^2 T}{\partial y^2}\right)$.
- The source term: $\frac{\Phi}{c_p}$. Term that would be considered, for example, if there is anything inside the material or flow that generates heat.

As the problem defined does not have any internal source, this term is despised. Furthermore, as it is a two dimensional that does not involves the velocity, it can also be despised the convective term. Therefore, the previous equation can be rewritten into the next one:

$$\rho c_p \frac{\partial T}{\partial t} = \frac{\partial}{\partial x}\left(k \frac{\partial T}{\partial x}\right) + \frac{\partial}{\partial y}\left(k \frac{\partial T}{\partial y}\right) + S \tag{4.2}$$

Now we can proceed to its discretization in order to do its numerical resolution. To see how discretize the equations using the FVM refer to section 3.2.

If we use an implicit scheme for the time discretization, the equation 4.2 discretized has the following form:

$$\begin{aligned}\rho c_p \frac{T_P^{n+1} - T_P^n}{\Delta t} V_p = {} & k_e \left(\frac{T_E^{n+1} - T_P^{n+1}}{d_{PE}}\right)\Delta y - k_w \left(\frac{T_P^{n+1} - T_E^{n+1}}{d_{WP}}\right)\Delta y \\ & + k_n \left(\frac{T_N^{n+1} - T_P^{n+1}}{d_{PN}}\right)\Delta x - k_s \left(\frac{T_P^{n+1} - T_S^{n+1}}{d_{SP}}\right)\Delta x + S\Delta x \Delta y\end{aligned} \tag{4.3}$$

Once the discretization is made, it is more common and useful to rewrite it as in the equation 4.4. It is more useful because of in that way you already have the geometric coefficients to be able to solve the equation.

$$a_P T_P = a_W T_W + a_E T_E + a_S T_S + a_N T_N + b_P \tag{4.4}$$

Where,

$$a_E = \frac{k_e \Delta y}{d_{PE}} \tag{4.5a}$$

$$a_W = \frac{k_w \Delta y}{d_{WP}} \tag{4.5b}$$

$$a_N = \frac{k_n \Delta x}{d_{PN}} \tag{4.5c}$$

$$a_S = \frac{k_s \Delta x}{d_{SP}} \tag{4.5d}$$

$$b_P = S\Delta x\Delta y + \frac{\rho c_p T_P^n}{\Delta t}\Delta x\Delta y \tag{4.5e}$$

$$a_P = a_E + a_W + a_N + a_S + \frac{\rho c_p}{\Delta t}\Delta x\Delta y \tag{4.5f}$$

The term T_P^n means the temperature calculated at the previous instant, and the multiplication of $\Delta x \Delta y$ is the volume of the control volume.

Finally, once the equation has been discretized and the geometric coefficients has been found, it is only need to solve the equation systems as it has explained in earlier word (in section 3.5) and use one of the explained solvers.

4.1.3. Analysis of the results

The simulation has been performed using a time step of $\Delta t = 0.50\ s$, and using a mesh of 60x40 nodes.

The simulation results can be seen in the figure 4.2. Observe that the material is heated by the right wall and also limited by the constant temperature at the bottom wall (that it is always constant at 23ºC). Furthermore, as the temperature of the right wall increases over the time the steady state is not reached.

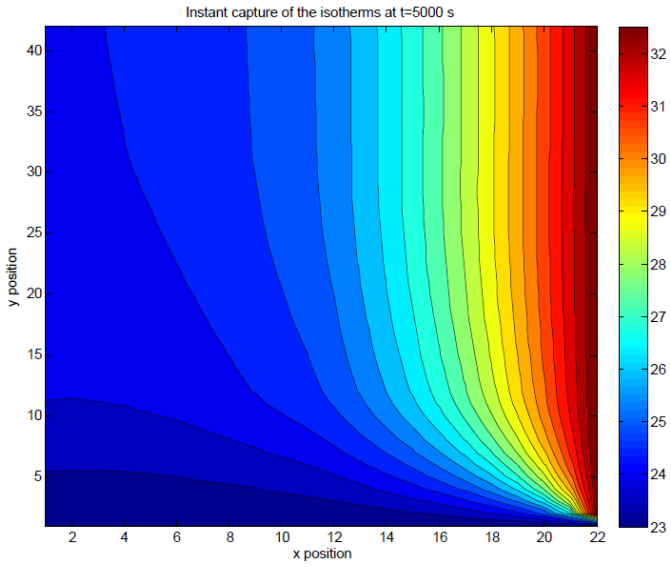

Figure 4.2 - Temperature solution at t=10000/2 s.

4.2. Smith-Hutton problem

The aim of this problem is to get familiar with the resolution of the convection. Besides it is a very good way to implement and test the numerical schemes (explained in the section 3.3) that are needed to evaluate the velocities at the control volume faces.

4.2.1. Definition of the problem

The Smith-Hutton is a two-dimensional convection and diffusion problem where the velocity field is given. As the velocity field is known there is no need to solve the Navier-Stokes equations, but also the convection-diffusion equation has to.

This problem consists in a rectangular cavity where the velocity is a solenoid flow, given by:

$$u(x,y) = 2y(1-x^2) \tag{4.6a}$$

$$v(x,y) = -2x(1-y^2) \tag{4.6b}$$

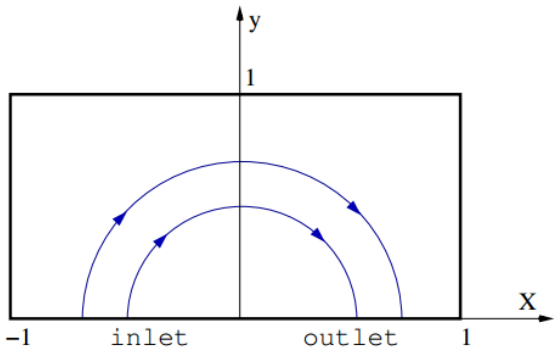

Figure 4.3 - Schema of Smith-Hutton problem.
Retrieved image from CTTC courses notes [https://www.cttc.upc.edu/].

4.2.2. Boundary conditions

The boundary conditions for the variable ϕ are defined in the next table. The α has the value of 10 and constant.

Table 4.4 - Boundary conditions of Smith-Hutton problem.

Boundary condition	Position
$\phi = 1 + \tanh\big(\alpha(2x+1)\big)$	$y = 0;\ \ x \in (-1,0) \qquad (inlet)$
$\dfrac{\partial \phi}{\partial y} = 0$	$y = 0;\ \ x \in (0,1) \qquad (outlet)$
$\phi = 1 - \tanh(\alpha)$	$(elsewhere)$

4.2.3. Mesh

The mesh used in this problem is uniform, as it can be seen in the figure 4.4 where is represented the grid of 40x40 nodes. The nodes are situated in the centre of the control volume, and also there are additional nodes at the faces of the boundary walls in order to get a better solution.

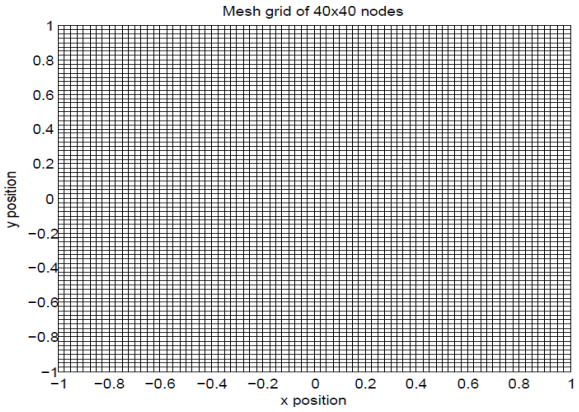

Figure 4.4 - Uniform mesh grid for Smith-Hutton problem (40x40 nodes).

4.2.4. Mathematical formulation of the problem

To solve the described problem, the convection-diffusion (equation 3.8) has to be solved. Rewriting it,

$$\frac{\partial(\rho\phi)}{\partial t} + \nabla(\rho\vec{u}\phi) = \nabla(\Gamma\nabla\phi) + S \tag{4.7}$$

To do so, it has been used the Finite Volume Method (FVM), as it has been explained in the section 3.2. Therefore, the discretization of the convection-diffusion equation is:

$$\left(\frac{\partial\rho\phi}{\partial t}\right)_P \cdot V_P + ((\dot{m}\phi)_e - (\dot{m}\phi)_w)\Delta y + ((\dot{m}\phi)_n - (\dot{m}\phi)_s)\Delta x = \left(\Gamma\frac{\partial\phi}{\partial x}S\right)_e - \left(\Gamma\frac{\partial\phi}{\partial x}S\right)_w + \left(\Gamma\frac{\partial\phi}{\partial y}S\right)_n - \left(\Gamma\frac{\partial\phi}{\partial y}S\right)_s \tag{4.8}$$[9]

Once the equation is discretized, it can be seen that there are some terms that cannot be evaluated directly.

- To determine the value of ϕ at each control volume face it is needed one of the numerical scheme that have been explained in the section 3.3, like a central difference scheme or an upwind difference scheme.

[9] Notice that the source term has been omitted because in this problem is not involved.

- For the evaluation the conductive flux $\left(\frac{d\phi}{dx}\right)$ for each face it can be used the arithmetic mean, such as represented for the west and east faces in the equation 4.9.

$$\left(\frac{d\phi}{dx}\right)_w = \frac{\phi_P - \phi_W}{d_{WP}} \quad (4.9a)$$

$$\left(\frac{d\phi}{dx}\right)_e = \frac{\phi_E - \phi_P}{d_{PE}} \quad (4.9b)$$

- For the time derivative term it is used a central difference scheme (CDS), as it is shown in the next equation 4.10.

$$\left(\frac{\partial \rho\phi}{\partial t}\right)_P \cdot V_P = \rho_P \frac{\phi_P^{n+1} - \phi_P^n}{\Delta t} V_P \quad (4.10)$$

Once the last three points are done, it is only needed to obtain the algebraic equation for each control volume following the next expression, the equation 4.11, in order to find the geometric coefficients.

$$a_P\phi_P = a_W\phi_W + a_E\phi_E + a_S\phi_S + a_N\phi_N + b_P \quad (4.11)$$

Where the coefficients are:

$$a_W = D_w \cdot A(|Pe_w|) + \max(-F_e, 0) \quad (4.12a)$$

$$a_E = D_e \cdot A(|Pe_e|) + \max(F_w, 0) \quad (4.12b)$$

$$a_S = D_s \cdot A(|Pe_s|) + \max(F_s, 0) \quad (4.12c)$$

$$a_N = D_n \cdot A(|Pe_n + \max(-F_n, 0) \quad (4.12d)$$

$$a_P = a_W + a_E + a_S + a_N + \frac{{\rho_P}^n}{\Delta t} V_P \quad (4.12e)$$

$$b_P = \frac{{\rho_P}^n {\phi_P}^n}{\Delta t} V_P \quad (4.12f)$$

Where,

$$D_e = \frac{\Gamma_e \Delta y}{d_{PE}} \qquad D_w = \frac{\Gamma_w \Delta y}{d_{WP}} \qquad D_s = \frac{\Gamma_s \Delta x}{d_{SP}} \qquad D_n = \frac{\Gamma_n \Delta x}{d_{PN}} \quad (4.13)$$

$$F_e = (\rho u)_e \Delta y \quad F_n = (\rho u)_n \Delta y \quad F_s = (\rho v)_s \Delta x \quad F_n = (\rho v)_n \Delta x \quad (4.14)$$

And the Peclet number ($Pe = \frac{F}{D}$) evaluated at the face of the control volume, has to be calculated depending on the numerical method used. Please refer to the table 4.5 to see how to evaluate it.

Table 4.5 - Values of A(|P|) for different numerical schemes.

Numerical scheme	$A(\|P\|)$
UDS	1
CDS	$1-0.50(\|P\|)$
HDS	$max(0,(1-0.5(\|P\|))$
EDS	$\|P\|/(e^{\|P\|}-1)$

Finally, when the coefficients are found, it is only needed to use a solver, one of those that have been explained in the section 3.5, in order to find the solution of the problem

4.2.5. Comparison of results

The aim of this section is to verify the simulated results comparing them with the reference results [13].

The next figure, number 4.5, shows the numerical results simulated for each ρ/Γ compared with the benchmark solution, each one as a function of the x-coordinate. The figure includes the three simulations, for ρ/Γ =10, 10^3 and 10^6.

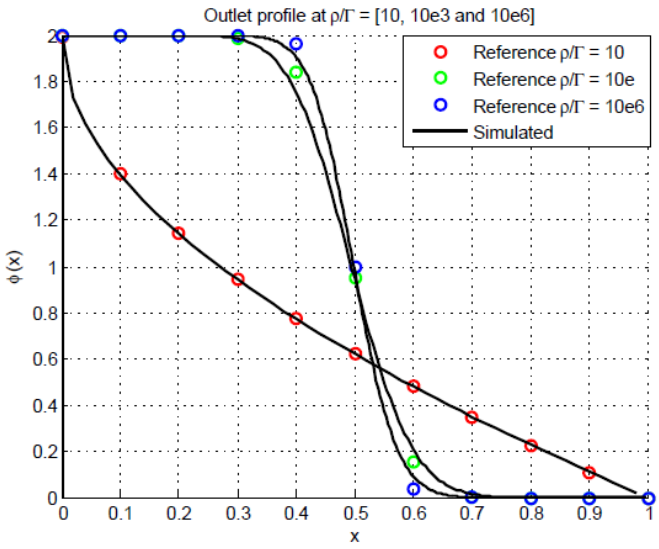

Figure 4.5 - SH. Comparison between the benchmark and the simulated solution.

For further information, please refer to Annex B, where there is a detailed comparison between the benchmark and the simulated solution. Furthermore, there is a study of mesh of this particular case.

4.2.6. Results

Once the simulated results have been verified it is time to plot those results and thereafter analyse its behaviour depending on the value of ρ/Γ.

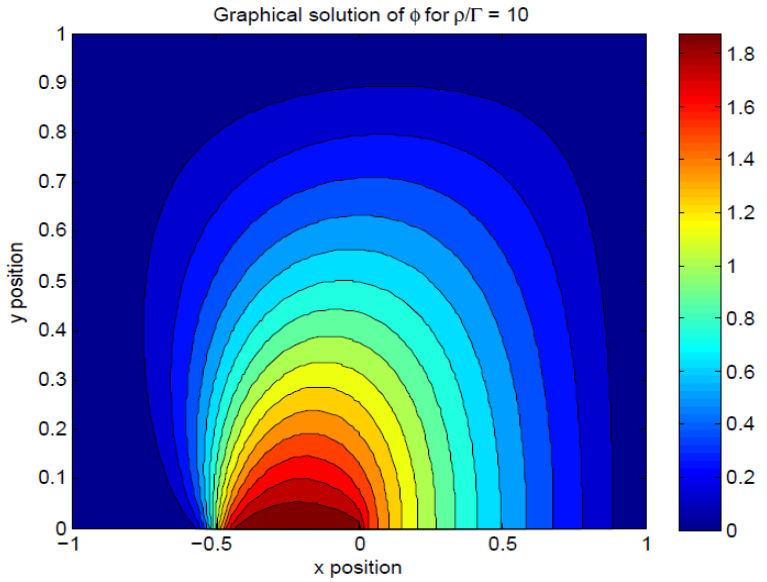

Figure 4.6 - SH. Graphical solution using CDS and ρ/Γ=10.

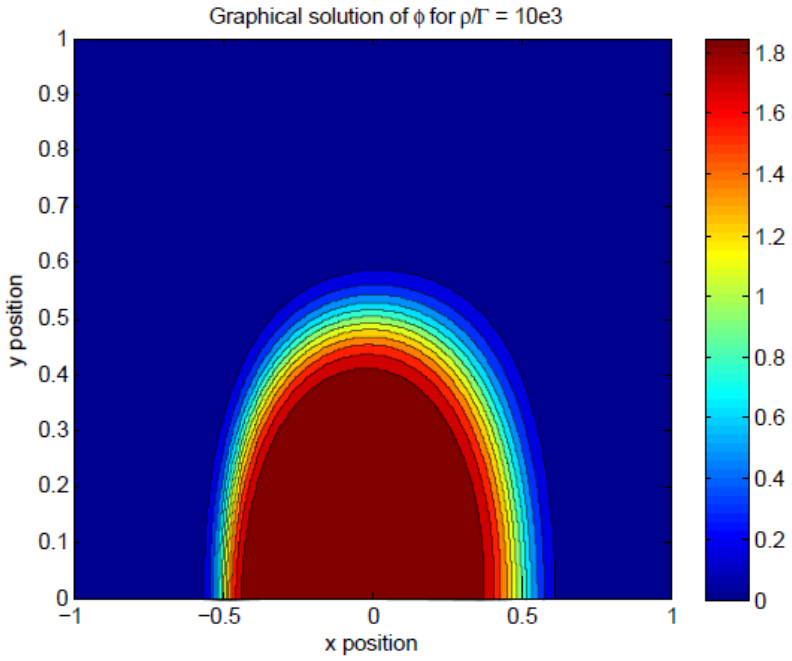

Figure 4.7 - SH. Graphical solution using CDS and ρ/Γ=10^3.

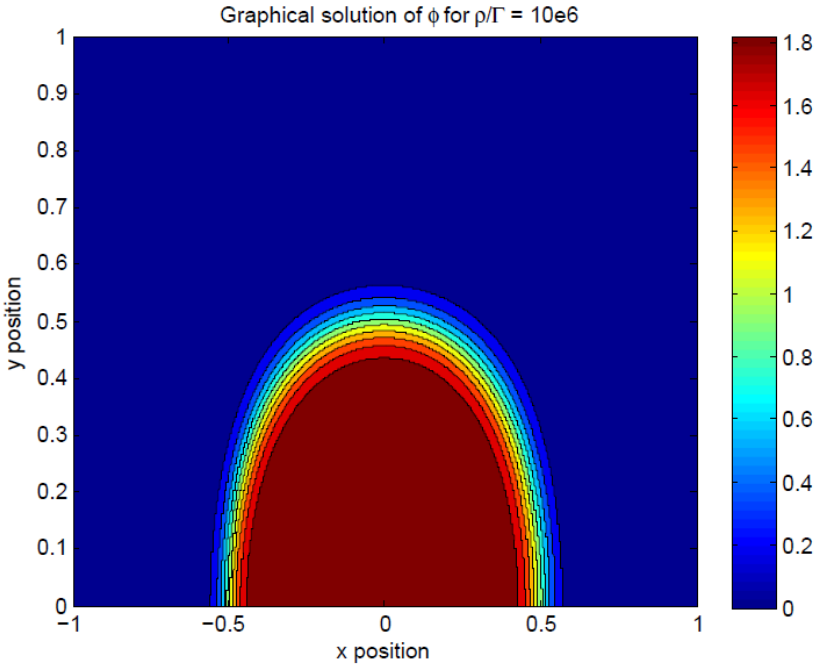

Figure 4.8 - SH. Graphical solution using CDS and ρ/Γ= 10⁶.

4.2.7. Analysis of the results

To solve this problem, the Convection-Diffusion equation has to be solved, which can be found previously in the equation 4.7. The Peclet number is directly related with the relationship ρ/Γ.

In the previous results obtained for this problem have been tested for 3 different Peclet number. If we analyses the convection-diffusion equation and we increase the Peclet number, the convective term increases too, but the diffusive decreases.

So, taking a look of the simulated figures, it can be appreciated how in the first figure the velocity enters in the cavity and by diffusion is dispersed through the cavity. But, in the others figures, where the Peclet has been increased, the diffusive term does not affect that much and the velocity enters in the cavity and goes off by convection.

In conclusion, if the Peclet increases the convective term is the dominants over the diffusive one, or vice versa if the Peclet number decreases.

4.3. Driven Cavity problem

The Driven-cavity problem (also known as lid-driven cavity), is a well know problem used to test or validate a new codes or new solution methods modelled to solve the Navier-Stokes equations. This problem consists of a two-dimensional viscous flow inside a square cavity (L for each broadside). Also it has infinite width, so to solve it, it can be consider as a 2D case.

4.3.1. Definition of the case

The aim of the problem is find the velocity field and the pressure at every different point of the cavity, as a function of the Reynolds number.

The known data of the problem are the boundaries conditions, as the pressures and the velocities in every wall of the cavity. As it may be seen in the next figure 4.9, all the velocities are zero, except in the top of the cavity where the velocity in the x direction is constant and equal to 1m/s. All the other walls can be considered static. Apart from the known velocities, on the walls we also known the pressure gradients (indicated on the next figure).

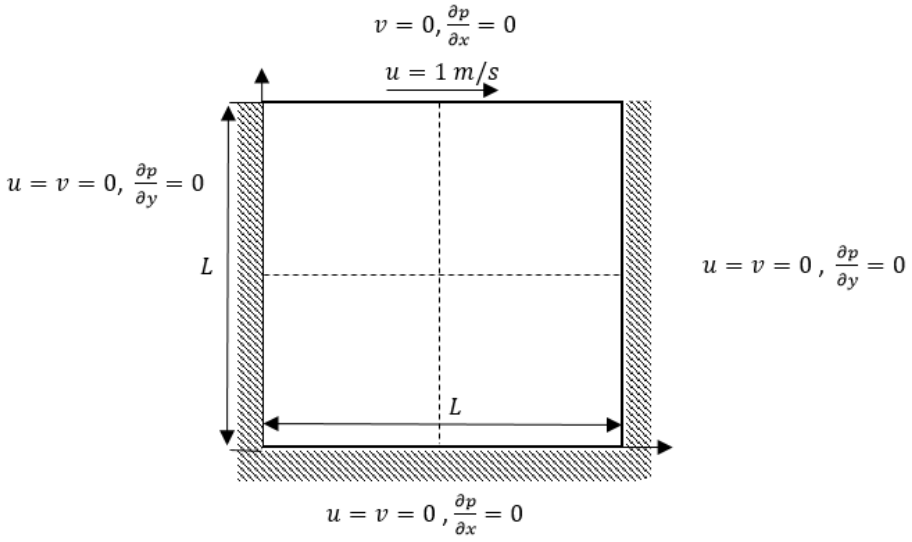

Figure 4.9 - Schema of the Driven Cavity problem.

4.3.2. Physical characteristics

The physical parameters that are needed in this problem are:

- The density of the fluid, which it has been fixed to $\rho = 1.00\ kg/m^3$.
- The dimensions of the cavity, that from the last figure 4.9 it can been seen that are L for each side.
- Velocity of the top wall of the cavity (u), which is equal to one.
- The dynamic viscosity μ that has been fixed with the Reynolds number as $\mu = \frac{1}{Re}$, in order to be the input parameter for each different Reynolds analyses.
- The dimensionless Reynolds number, which is an important parameter defined as $Re = \frac{\rho UL}{\mu}$. Where this case the value of U is the velocity of the top wall, and it is going to be the changing parameter.

4.3.3. Mesh

In order to get a more accuracy solution, the mesh is thinner near the walls. To do so, it is used a refined mesh. The most common way to generate a refined mesh is by using the hyperbolic tangent for each coordinate, as is defined in the next equations:

$$x = \frac{Lx}{2}\left(1 + \frac{\tanh\left(\gamma\left(\frac{2\cdot i}{Nx+1} - 1\right)\right)}{\tanh\gamma}\right) \tag{4.15a}$$

$$y = \frac{Ly}{2}\left(1 + \frac{\tanh\left(\gamma\left(\frac{2\cdot j}{Ny+1} - 1\right)\right)}{\tanh\gamma}\right) \tag{4.15b}$$

The result of this formulation is illustrated in the next figure 4.10, with a thinner grid near the walls with the aim to make a better approximate near the walls.

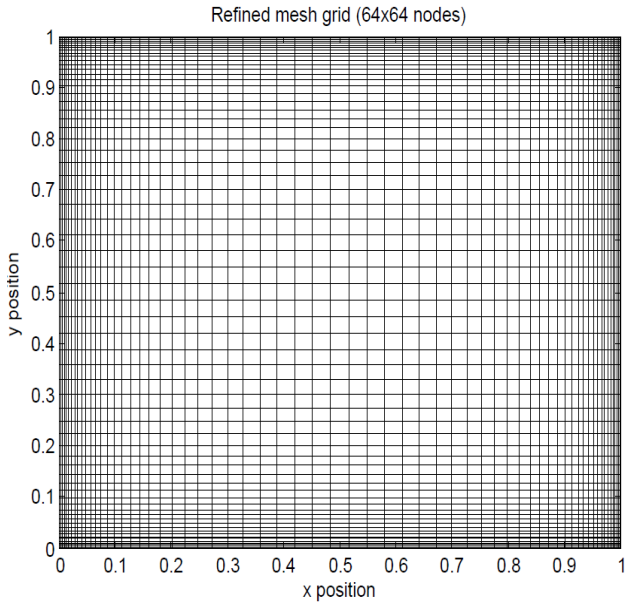

Figure 4.10 - Mesh formulation for Driven Cavity problem. Grid of 64x64 nodes.

4.3.4. Mathematical formulation of the problem

As it has been said in the previous introduction to this problem, the Navier-Stokes equations have to be solved. To do so, it is used the Fractional Step Method (FSM).

To see in more detail how the resolution of this problem has been developed, in this section are explained the used discretization equations.

Such it was commented in the section 3.4.3 where the checkerboard problem is explained. To solve the FSM correctly, it will be needed to solve the velocities in the staggered meshes (the u velocity in the staggered mesh x, and the v velocity in the staggered mesh y). And the pressures will be solved at the centred mesh.

In the following explanations is described point by point how it has been solved the problem.

First, it is need to do the evaluation of $R(u^n)$. As the dynamic viscosity of the problem it has been considered constant and fixed by the Reynolds number: $\mu = \frac{1}{Re}$. The discretization of the convective and the diffusive terms is the following one:

$$R(u^n) = \frac{1}{Re}\left[\frac{u_E - u_P}{d_{PE}}\Delta y - \frac{u_P - u_W}{d_{WP}}\Delta y + \frac{u_N - u_P}{d_{PN}}\Delta x - \frac{u_P - u_S}{d_{SP}}\Delta x\right] - [(\rho u)_e u_e \Delta y - (\rho u)_w u_w \Delta y + (\rho v)_n u_n \Delta x - (\rho v)_s u_s \Delta x] \quad (4.16)$$

And, the diffusive and convective term has to be evaluated for the vertical velocity component as:

$$R(v^n) = \frac{1}{Re}\left[\frac{v_E - v_P}{d_{PE}}\Delta y - \frac{v_P - v_W}{d_{WP}}\Delta y + \frac{v_N - v_P}{d_{PN}}\Delta x - \frac{v_P - v_S}{d_{SP}}\Delta x\right] - [(\rho u)_e v_e \Delta y - (\rho u)_w v_w \Delta y + (\rho v)_n v_n \Delta x - (\rho v)_s v_s \Delta x] \quad (4.17)$$

As it has been said before, the velocity are evaluated at the control volume faces. Doing so, the $R(u^n)$ term is evaluated at the staggered x mesh and the $R(v^n)$ term in the staggered y mesh. Once that is understand, it is needed to focus on how the mass flow and velocities at the faces are evaluated. Below are explained how to evaluate this two parameters. Please refer to illustrations to understand more clearly its determination.

Evaluation of the velocities u_w, u_e, u_n and u_s, in the mass flow calculation:

In order to calculate the mass flow (ρu) evaluated at each face of the control volume it is convenient to pay attention to the figure 4.11. In the figure it is showed the velocities in each staggered mesh and its neighbour's velocities.

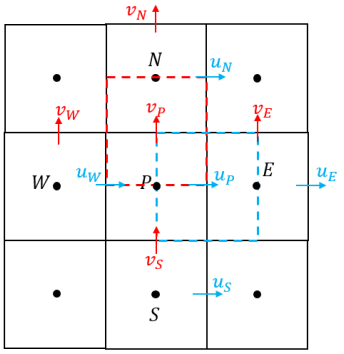

Figure 4.11 - Velocities formulation in the staggered meshes.

Therefore, the mass flow will be calculated by making the average velocity at each face. For example, in the next four equations it is showed how to calculate the mass flows for the staggered horizontal mesh.

$$(\rho u)_w = \rho \cdot 0.50 \cdot (u_W + u_P) \quad (4.18)$$

$$(\rho u)_e = \rho \cdot 0.50 \cdot (u_E + u_P) \quad (4.19)$$

$$(\rho u)_e = \rho \cdot 0.50 \cdot (u_N + u_P) \quad (4.20)$$

$$(\rho u)_e = \rho \cdot 0.50 \cdot (u_S + u_P) \quad (4.21)$$

Evaluation of u_w, u_e, v_n, and v_s in the horizontal staggered mesh:

In the equations 4.16 and 4.17 it is also needed to evaluate the velocity at the faces of the staggered mesh. To see how this works, look at the figure 4.12 where it is illustrated the staggered mesh in the horizontal direction.

Following this scheme, and using the CDS[10], the velocities at the faces in the horizontal staggered mesh, are:

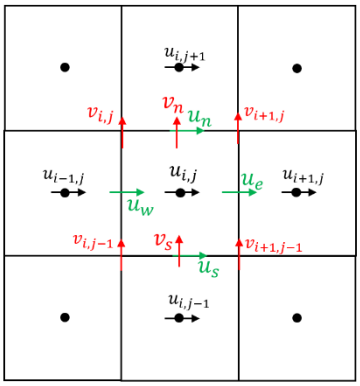

Figure 4.12 - Velocity formulation in the staggered x mesh.

$$u_w = 0.50 \cdot (u_{i,j} + u_{i-1,j}) \quad (4.22)$$

$$u_e = 0.50 \cdot (u_{i+1,j} + u_{i,j}) \quad (4.23)$$

And the vertical velocities in the staggered horizontal mesh, using CDS, are:

$$v_n = 0.50 \cdot (v_{i,j} + v_{i+1,j}) \quad (4.24)$$

$$v_s = 0.50 \cdot (v_{i,j-1} + u_{i+1,j-1}) \quad (4.25)$$

Secondly, once the $R(u^n)$ and $R(v^n)$ are calculated, it can be found the predictor velocity, for each component. See the next equations.

$$u^p = u^n + \frac{\Delta t}{V_P}\left(\frac{3}{2}R(u^n) - \frac{1}{2}R(u^{n-1})\right) \quad (4.26)$$

$$v^p = v^n + \frac{\Delta t}{V_P}\left(\frac{3}{2}R(v^n) - \frac{1}{2}R(v^{n-1})\right) \quad (4.27)$$

Thirdly, it is needed to solve the Poisson equation:

$$\left(\frac{p_E^{n+1} - p_P^{n+1}}{d_{EP}} - \frac{p_P^{n+1} - p_W^{n+1}}{d_{PW}}\right)\Delta y + \left(\frac{p_N^{n+1} - p_P^{n+1}}{d_{NP}} - \frac{p_P^{n+1} - p_S^{n+1}}{d_{PS}}\right)\Delta x = \frac{1}{\Delta t}[(\rho u^p)_e \Delta y - (\rho u^p)_w \Delta y + (\rho u^p)_n \Delta x - (\rho u^p)_s \Delta x] \quad (4.28)$$

To solve the equation 4.28 it will be used one of the solvers explained in the section 3.5, but firstly it is needed to put the Poisson equation as a system of algebraic equations as it was showed below.

$$a_P p_P^{n+1} = a_W p_W^{n+1} + a_E p_E^{n+1} + a_N p_N^{n+1} + a_S p_S^{n+1} + b_P \quad (4.29)$$

$$a_W = \frac{\Delta y}{d_{PW}} \quad (4.30a)$$

(4.30b)

[10] It is used CDS as a simple example. Once the mass flow is calculated it can be used any other numerical scheme as the ones explained in the section 3.3.

$$a_E = \frac{\Delta y}{d_{EP}} \quad (4.30c)$$

$$a_N = \frac{\Delta x}{d_{NP}} \quad (4.30d)$$

$$a_S = \frac{\Delta x}{d_{PS}} \quad (4.30e)$$

$$b_P = -\frac{1}{\Delta t}[(\rho u^p)_e \Delta y - (\rho u^p)_w \Delta y + (\rho u^p)_n \Delta x - (\rho u^p)_s \Delta x]$$

And finally, it calculated the new velocity by the next equations:

$$u^{n+1} = u^p - \Delta t \left(\frac{p_B - p_A}{d_{BA}}\right) \quad (4.31)$$

$$v^{n+1} = v^p - \Delta t \left(\frac{p_B - p_A}{d_{BA}}\right) \quad (4.32)$$

4.3.5. Comparison of results

In order to verify the results obtained by the simulation of the code, the next images are made to compare easily with view, the reference solution [14] with the simulated solution. However, to see more information about the used mesh, refer to the Annex C.1 to see the mesh study for this problem.

The simulation has been made for different Reynolds number, from 100 to 7500. Later is going to be analysed how the results change as a function of the Reynolds number.

In the next figures the u velocities are plot along the vertical line thought the geometric centre of the cavity, and the v velocities are plot along the horizontal x line thought the geometric centre of the cavity. In both cases the solid blue line belongs to the simulated solution, and the red points belong to the reference solution.

Re=100: Using a mesh of 64x64.

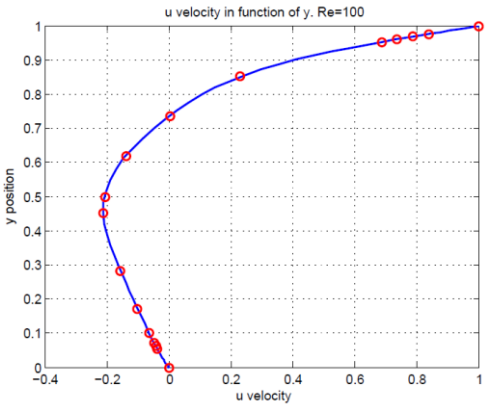

Figure 4.13 - DC, velocity u comparison Re=100.

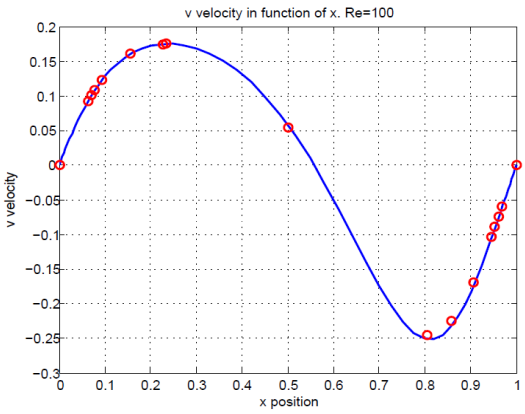

Figure 4.14 - DC, velocity v comparison. Re=100.

Re=400: Using a mesh of 64x64

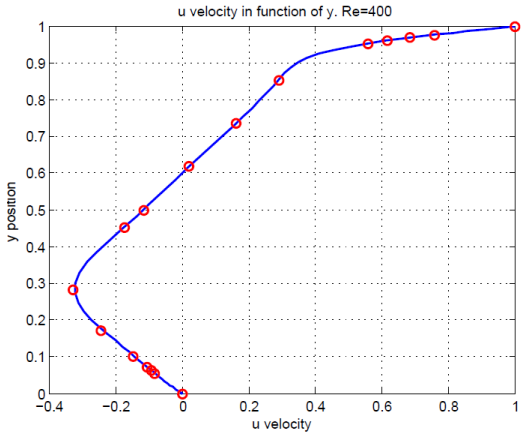

Figure 4.15 - DC, velocity u comparison. Re=400.

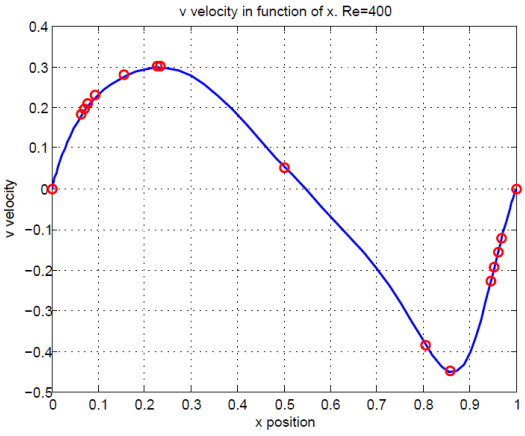

Figure 4.16 - DC, velocity v comparison. Re=400.

Re=1000: Using a mesh of 64x64 nodes.

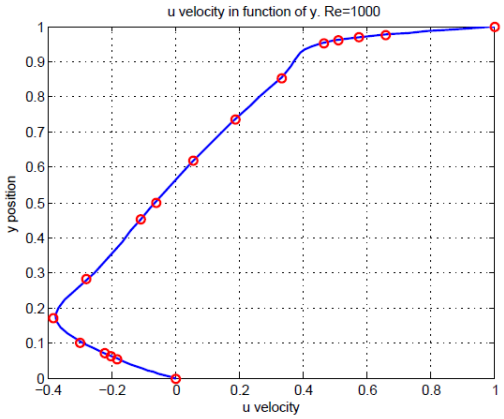

Figure 4.17 - DC, velocity u comparison Re=1000.

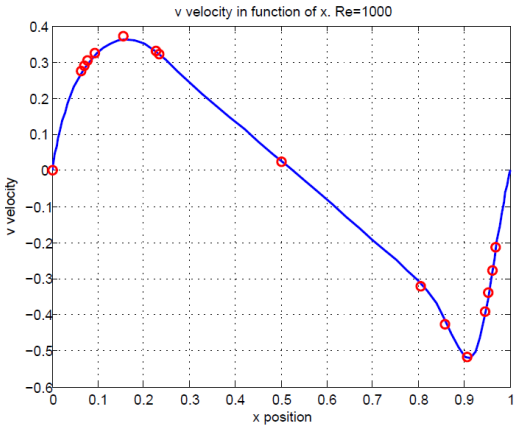

Figure 4.18 - DC, velocity v comparison Re=1000.

Re=3200: Using a mesh of 64x64 nodes.

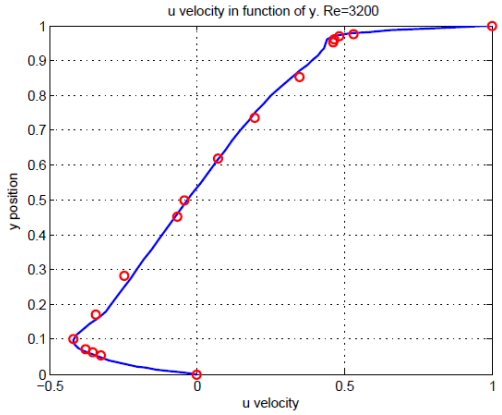

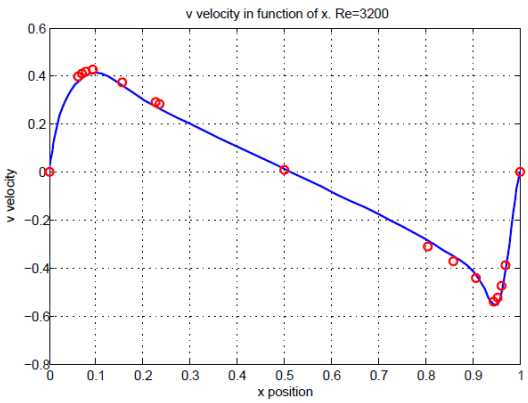

Figure 4.19 - DC, velocity u comparison Re=3200.

Figure 4.20 - DC, velocity v comparison Re=3200.

Re=5000: Using a mesh of 64x64 nodes.

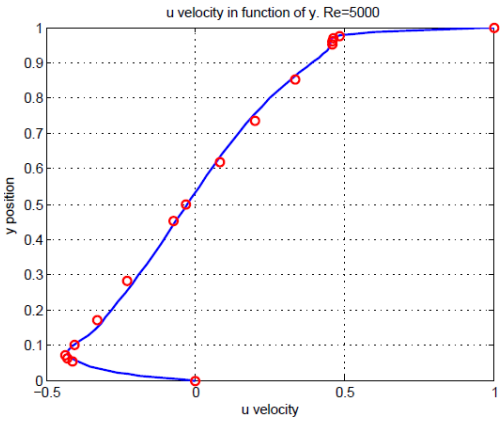

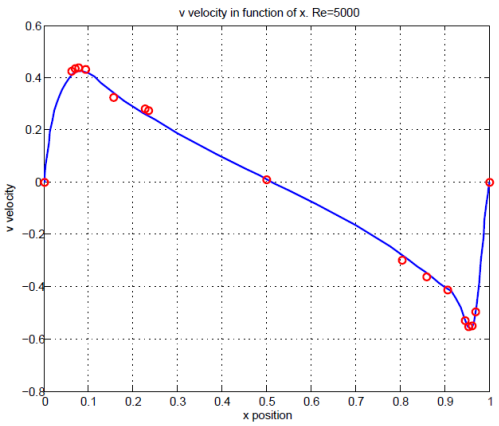

Figure 4.21 - DC, velocity u comparison Re=5000.

Figure 4.22 - DC, velocity v comparison Re=5000.

Re=7500: Using a mesh of 64x64 nodes.

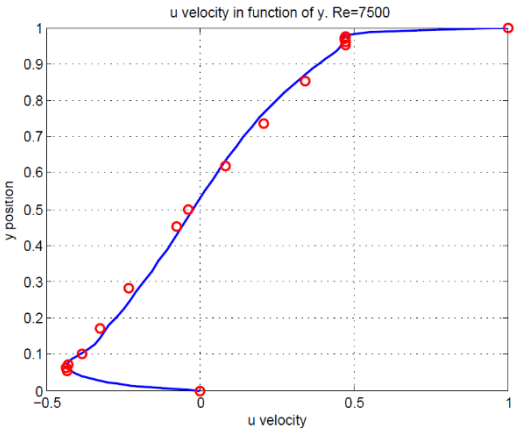

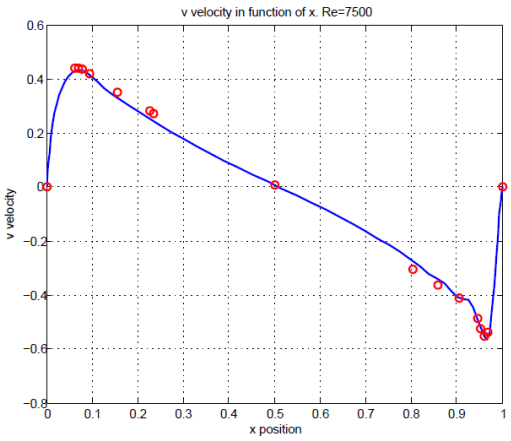

Figure 4.23 - DC, velocity u comparison Re=7500.

Figure 4.24 - DC, velocity v comparison Re=7500.

However, even the comparison figures 4.23 and 4.24 are certainly correct, for Reynolds numbers higher than 7200 it may appear some stability problems with the solution. To do so, the time step has been reduced to $\Delta t = 0.001\ s$.

In the next graph, you can see the time evolution of the horizontal velocity at the geometric centre of the cavity.

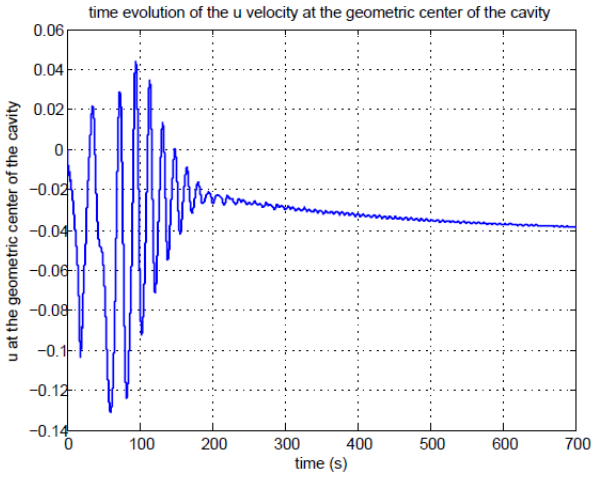

In the left graph (figure 4.25), it is shown the time evolution of the horizontal component of the velocity (u) located in the centre of the cavity (x and y both at the centre)

Note that what this image wants to illustrate is the convergence of the code.

Figure 4.25 - DC. Time evolution of u velocity for Re=7500.

As it can be seen from 0 to 200s it seems to have a high unsteady behaviour, but above 200s it seems to begin to stabilize (by start approaching to a constant value). The illustrated simulation has been converge in 700s. Nevertheless, if a zoom from 640 to 680s is made, we can see that it is not really true.

To see more detail of this behaviour, please refer to figure 4.26, where a zoom of the figure 4.25 is illustrated. Observe that the velocity remains oscillating without tending to a constant value. In other words, for high Reynolds like 7500 it stills being in the laminar zone, although it does not exist a steady solution.

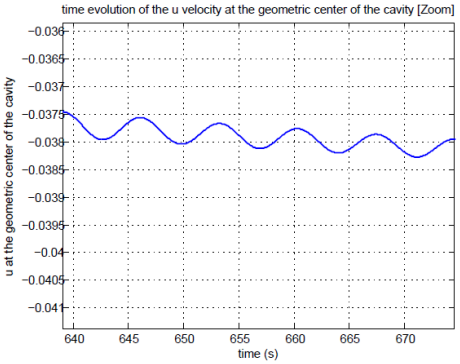

Figure 4.26 - DC. Time evolution of u velocity for Re=7500. [Zoom between 640-680 s].

As a matter of fact, in the literature it can be found some studies that prove this behaviour that in high Re numbers the solution is unsteady. Please see references [15] and [16].

4.3.6. Results

Once the numerical results simulated have been compared with the correct results and are considered valid. It is time to plot the simulated results for the most representative Reynolds numbers and make an analysis how the increase of this number affects.

In the next figures are represented the velocities contours and the streamlines that are created inside of the cavity. There are only the results for the Reynolds numbers of 100, 1000 and 5000. To see the rest of results for the rest of Reynolds numbers simulated please refer to Annex C.2.

Re=100:

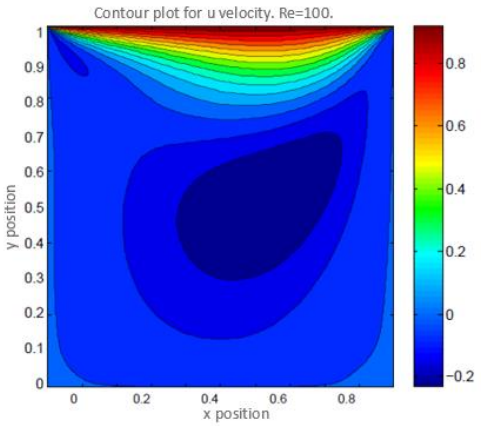

Figure 4.27 - DC, u velocity. Re=100.

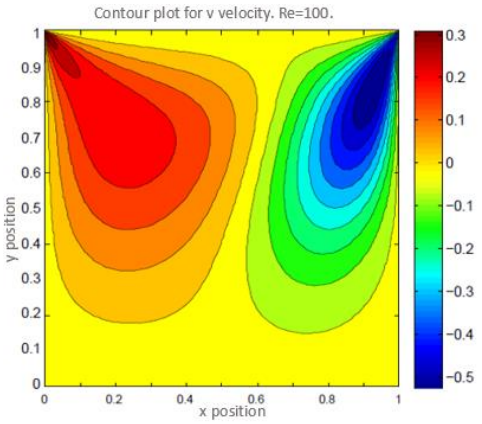

Figure 4.28 - DC, v velocity. Re=100.

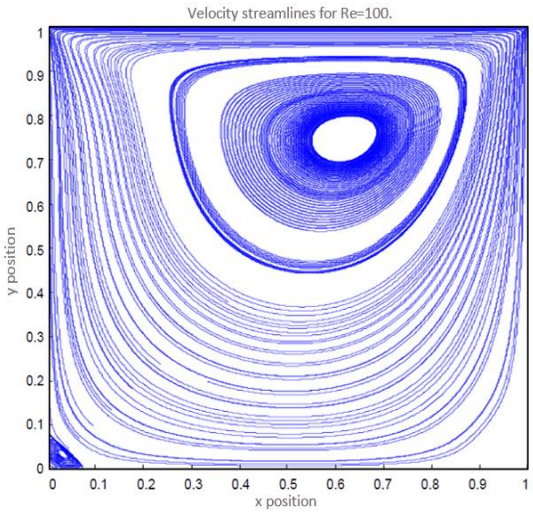

Figure 4.29 - DC. Velocity streamlines. Re=100.

Re=1000: Using a 100x100 grid

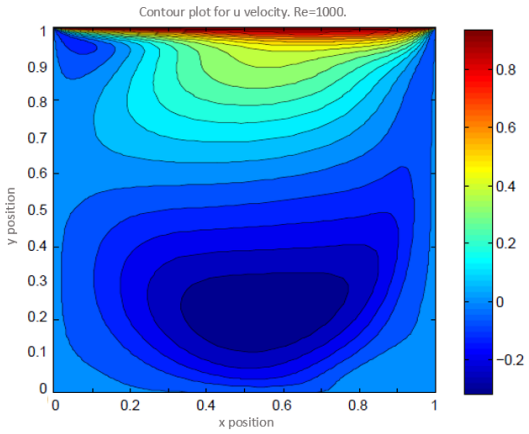

Figure 4.30 - DC, u velocity. Re=1000.

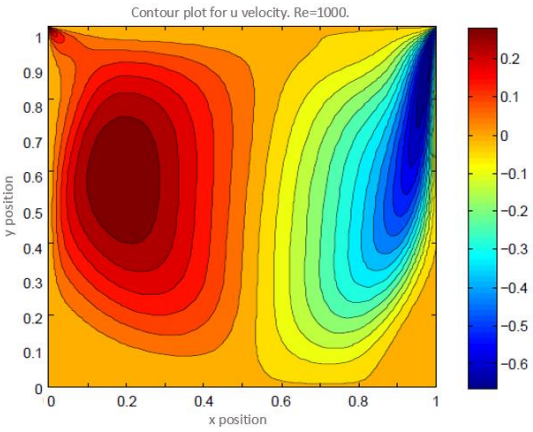

Figure 4.31 - DC, v velocity. Re=1000.

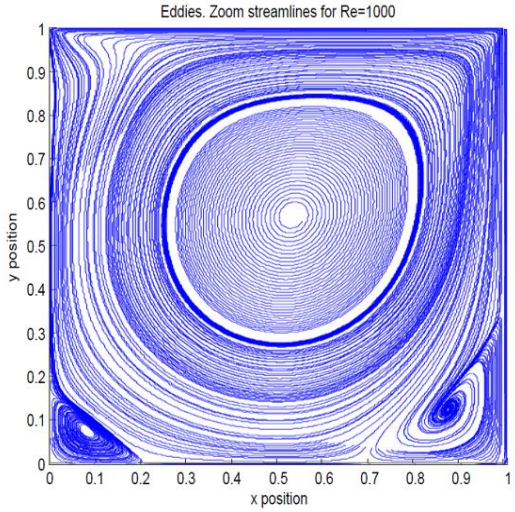

Figure 4.32 - DC. Velocity streamlines. Re=1000.

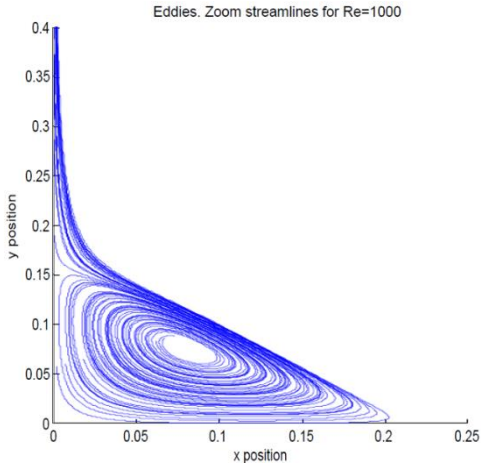

Figure 4.33 - DC. Bottom left wall eddy. Re=1000.

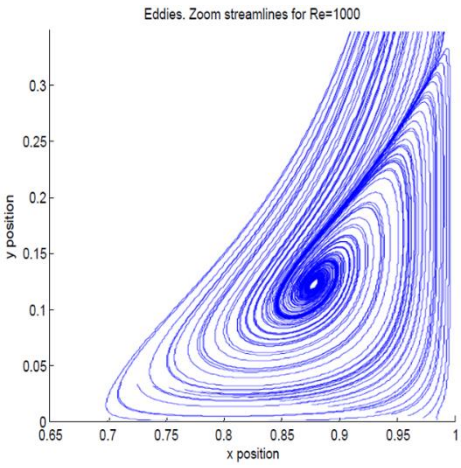

Figure 4.34 - DC. Bottom right wall eddy. Re=1000.

Re=5000: Using a mesh of 64x64 nodes.

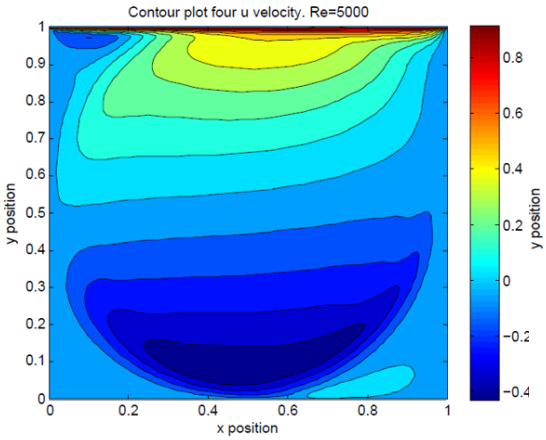

Figure 4.35 - DC, u velocity. Re=5000.

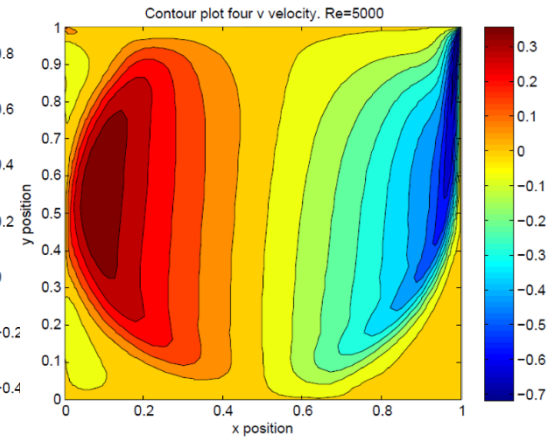

Figure 4.36 - DC, v velocity. Re=5000.

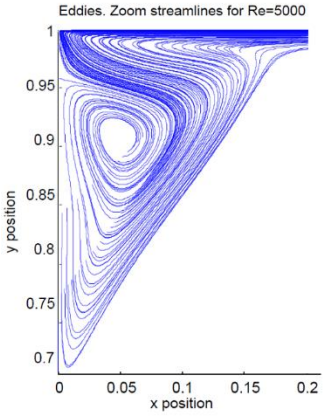

Figure 4.37 - DC. Top left wall eddy. Re=5000

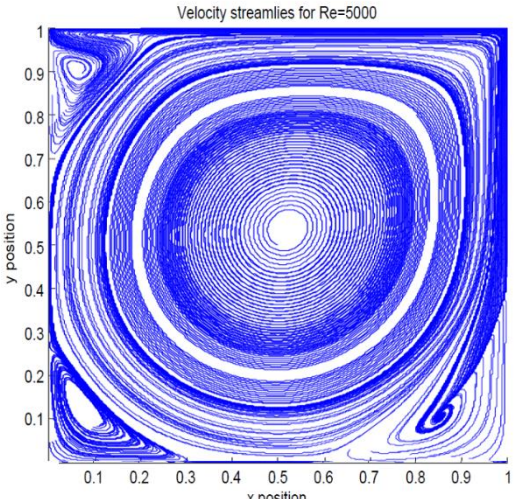

Figure 4.38 - DC. Velocity streamlines, Re=5000.

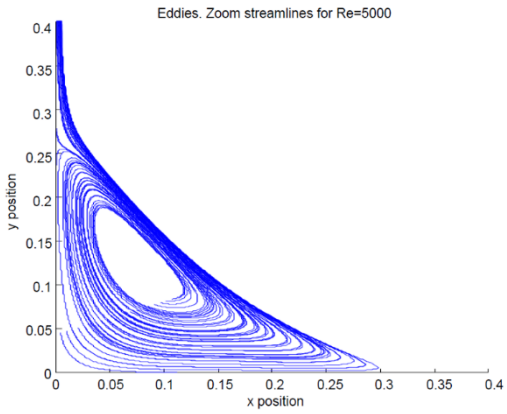

Figure 4.39 - DC. Bottom left wall eddy. Re=5000.

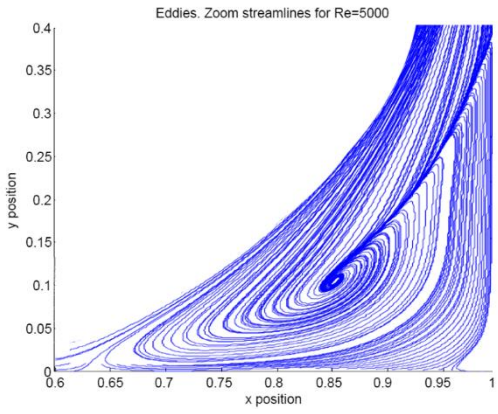

Figure 4.40 - DC. Bottom right wall eddy. Re=5000.

4.3.7. Analysis of the results and conclusions

With the aim of understand how the driven cavity flow behaves, we are going to analyse in more detail the results (previously illustrated), for each Reynolds number.

In the first place, for Reynolds number 100 the dominant forces are the viscous ones, meaning that the convective term has almost no influence. So, as it can be seen in the velocity streamlines for this case (figure 4.29) the flow has no enough force to create a perfect rotation inside the cavity. That happens because the diffusive term erase that energy from the velocity reference.

In the second place, if the Reynolds number is increased to 1000. In this case the velocity streamlines (figure 4.32) shows how the eddy begins to be centred inside the cavity, but also not completely. Which means that the convective forces start showing. Furthermore, it starts appearing two vortex near the bottom walls, which are showed in more detail in the figures 4.33 and 4.34.

Thirdly, for a Reynolds number of 5000, the dominant term is clearly the convective. If the streamlines velocity for this case are seen (figure 4.38), as a difference from the previous Reynolds analyse, the eddy is completely centred inside the cavity. Moreover, it appears a third vortex near the left top wall (see figure 4.37) and the two that have already appeared in the Re=100 are defined even more clearly (figures 4.39 and 4.40).

Finally, using a Reynolds number of 7500 it has been seen how the solution starts being non steady, although the simulated values continue agreeing with the reference ones.

In conclusion, the Reynolds number make an important effect to the behaviour in forced convection cases. In this case, as it is clear from the explanations and figures given, for low Re the top velocity does not affect much due to the viscous forces are dominant and the eddy appears near the top wall. For a Re higher, the convective term begins to take force and the eddy is well centred inside the cavity as long as the Re is increased, and also it appears some vortex near the walls.

Moreover, for higher Re the kinematic viscosity tends to zero and that creates instability problems, that have been solved by decreasing the time step and waiting till de solution converges.

4.4. Differentially heated cavity problem

The *Differentially heated cavity problem* is a variation of the *Driven cavity problem*, that instead of generating the velocities and the movement inside the cavity by an external force, the movement is caused by the temperature difference inside the cavity. Therefore, the *Driven cavity* was a forced convection problem and the *Differentially heated cavity* is a natural convection problem.

4.4.1. Definition of the case

The problem consists in a two-dimensional[11] natural flow in a square cavity (as it is described next). The horizontal walls are insulated, and the vertical walls are at temperature T_{hot} on the left and T_{cold} on the right.

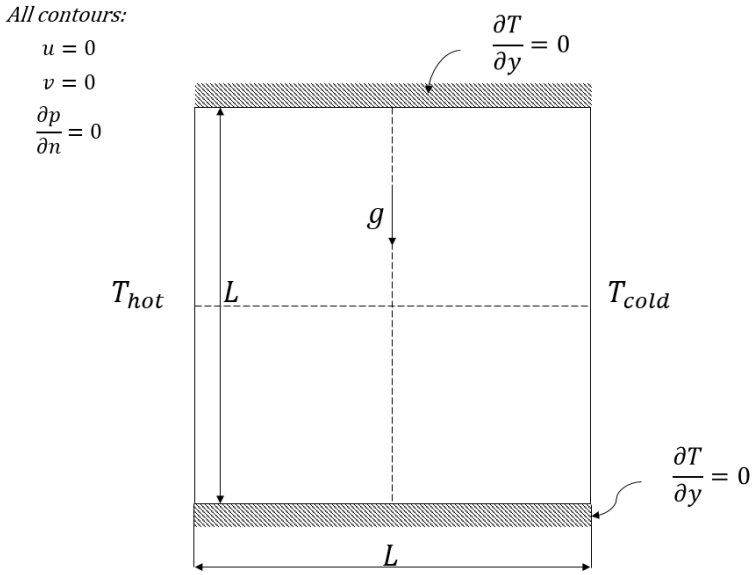

Figure 4.41 - Schema of Differentially Heated Cavity problem.

As it can be seen in the figure 4.41 the boundaries conditions for the cavity are:

- Null velocity on all walls, both components of the velocity.
- The derivative of pressure is null on all the walls.
- The top and bottom walls are adiabatic, which means the derivative of temperature is null.

[11] It has also an infinite width, so it would be treated as a 2D case.

4.4.2. Physical characteristics

The physical parameters and characteristics needed in this problem are:

- The dimensionless Prandtl number, defined as $Pr = \frac{c_p \mu}{k}$. As the used fluid is air its value is fixed to $Pr = 0.71$.
- The dimensionless Rayleigh number, defined as $Ra = \frac{\beta g L^3 \Delta T}{\nu^2} \frac{c_p \mu}{k} = \frac{\beta g L^3 \Delta T c_p \rho^2}{k\mu}$. It would be the changing parameter, in order to evaluate its effect.

4.4.3. Mesh

In this problem it were used two types of meshes: the uniform and the refined uniform mesh[12] near the walls, in order to see which one was better in this case.

4.4.4. Mathematical formulation of the problem

As it has been said in the introduction of this problem, it is a variation of the previous problem (the Driven cavity). Therefore, it has already been explained the methodology of how discretize the equations, the resolution of the FSM and how approximate the velocities at the faces. Even so, the mathematical formulation of the *Differentially Heated Cavity problem* it is explained next, by introducing the important modifications over the previous problem.

However, to see more clearly the non-dimensionalization of the Navier-Stokes equations in natural convection, please refer to Annex A.2.

First of all, the new is the temperature and the evaluation of the $R(T^n)$ term is defined in the equation 4.33.

$$R(T^n) = \left[\frac{T_E - T_P}{d_{PE}}\Delta y - \frac{T_P - T_W}{d_{WP}}\Delta y + \frac{T_N - T_P}{d_{PN}}\Delta x - \frac{T_P - T_S}{d_{SP}}\Delta x\right] - [(\rho u)_e T_e \Delta y - (\rho u)_w T_w \Delta y + (\rho v)_n T_n \Delta x - (\rho v)_s T_s \Delta x] \quad (4.33)$$

[12] The refined mesh was explained earlier in the Driven Cavity problem, please refer to section 4.3.1 to see it in more detail.

Then, following the NS equations considering natural convection, the evaluation of the $R(u^n)$ and $R(v^n)$ terms is the following equations 3.34 and 3.35.

$$R(u^n) = Pr\left[\frac{u_E - u_P}{d_{PE}}\Delta y - \frac{u_P - u_W}{d_{WP}}\Delta y + \frac{u_N - u_P}{d_{PN}}\Delta x - \frac{u_P - u_S}{d_{SP}}\Delta x\right] - [(\rho u)_e u_e \Delta y - (\rho u)_w u_w \Delta y + (\rho v)_n u_n \Delta x - (\rho v)_s u_s \Delta x] \quad (4.34)$$

$$R(v^n) = Pr\left[\frac{v_E - v_P}{d_{PE}}\Delta y - \frac{v_P - v_W}{d_{WP}}\Delta y + \frac{v_N - v_P}{d_{PN}}\Delta x - \frac{v_P - v_S}{d_{SP}}\Delta x\right] - [(\rho u)_e v_e \Delta y - (\rho u)_w v_w \Delta y + (\rho v)_n v_n \Delta x - (\rho v)_s v_s \Delta x] + +\mathrm{Pr}\, Ra\, T'\Delta x \Delta y \quad (4.35)$$

As it can be seen, the evaluation of the diffusive and convective term for the horizontal component of the velocity it is almost the same as before, with the only change that now the viscosity is fixed by the Prandtl number.

Even so, the evaluation of the mass flow and the velocities at the faces are such has been defined in earlier words in the section 4.3.

Once the convective and diffusive term is evaluated for the temperatures in all the problem domain, the temperature at the next instant can be found as it is shown in the equation 4.36.

$$T^{n+1} = T^n + \frac{\Delta t}{V_P}\left(\frac{3}{2}R(T^n) - \frac{1}{2}R(T^{n-1})\right) \quad (4.36)$$

Then, the predictor velocity, for each component of the velocity, is determined below in the equations 4.37 and 4.38.

$$u^p = u^n + \frac{\Delta t}{V_P}\left(\frac{3}{2}R(u^n) - \frac{1}{2}R(u^{n-1})\right) \quad (4.37)$$

$$v^p = v^n + \frac{\Delta t}{V_P}\left(\frac{3}{2}R(v^n) - \frac{1}{2}R(v^{n-1})\right) \quad (4.38)$$

The formulation of the Poisson equation is the same as before.

$$\left(\frac{p_E^{n+1} - p_P^{n+1}}{d_{PE}} - \frac{p_P^{n+1} - p_W^{n+1}}{d_{WP}}\right)\Delta y + \left(\frac{p_N^{n+1} - p_P^{n+1}}{d_{PN}} - \frac{p_P^{n+1} - p_S^{n+1}}{d_{SP}}\right)\Delta x = \frac{1}{\Delta t}[(\rho u^p)_e \Delta y - (\rho u^p)_w \Delta y + (\rho u^p)_n \Delta x - (\rho u^p)_s \Delta x] \quad (4.39)$$

And finally, the velocity correction is defined next.

$$u^{n+1} = u^p - \Delta t\left(\frac{p_B - p_A}{d_{BA}}\right) \quad (4.40)$$

$$v^{n+1} = v^p - \Delta t\left(\frac{p_B - p_A}{d_{BA}}\right) \quad (4.41)$$

4.4.5. Comparison results

In order to verify the developed code, in this section it is made a comparative between the benchmark solution [15] and the results obtained by the simulation. Each comparison is made for a different Rayleigh number, from 10^3 to 10^6.

The comparison parameters are defined next:

- u_{max}: is the maximum horizontal velocity on the vertical mid-plane of the cavity, and y is its location.
- v_{max}: is the maximum vertical velocity on the horizontal mid-plane of the cavity, and x is its location.
- $\overline{Nu}$: is the average Nusselt number throughout the cavity.
- Nu_{max}: is the maximum value of the local Nusselt number on the boundary at x=0 and y is its location.
- Nu_{min}: is the minimum value of the local Nusselt number on the boundary at x=0, and y is its location.

Where the local Nusselt number at the left wall (x=0) or the right wall (x=1) is:

$$Nu = \int_0^1 \frac{\partial T}{\partial x} dz \Big|_{x=0 \; or \; x=1} \tag{4.42}$$

In the next tables there is a comparative between the benchmark solution and the solutions obtained through the simulation, for each Rayleigh number: 10^3, 10^4, 10^5 and 10^6.

Table 4.6 - DHC. Comparison results for Ra=10e3.

$\boldsymbol{Ra = 10^3}$					
		Uniform 40x40 mesh		Refined 32x32 mesh	
	Benchmark solution	Results	Error (%)	Results	Error (%)
u_{max}	3.6490	3.6570	0.2192	3.6629	0.3807
y	0.8130	0.8125	0.0615	0.8085	0.5498
v_{max}	3.6970	3.6989	0.0514	3.7027	0,1553
x	0.1780	0.1875	5.3371	0.1915	7.5618
$\overline{Nu}$	1.1180	1.1220	0.3578	1.1424	2.1825
Nu_{max}	1.5050	1.5124	0.4917	1.5088	0.1242
y	0.0920	0.0875	4.8913	0.0934	1.5217
Nu_{min}	0.6920	0.6889	0.4480	0.6913	0.1015
y	1.0000	0.9875	1.2500	1.0000	0.0000

In the table 4.6 is compared the benchmark solution with the results obtained for Ra=10^3. The solution values seems to be correct for both used meshes, because its error is minimum.

Table 4.7 - DHC. Comparison results for Ra=10e4.

$Ra = 10^4$					
		Uniform 40x40 mesh		Refined 32x32 mesh	
	Benchmark solution	Results	Error (%)	Results	Error (%)
u_{max}	16.1780	16.141	0.2287	16.0816	0,5959
y	0.8230	0.8125	1.2758	0.8085	1.7618
v_{max}	19.6170	19.638	0.1071	19.7655	0.7570
x	0.1190	0.1125	5.4622	0.1200	0.8403
$\overline{Nu}$	2.2430	2.3603	5.2296	2.2004	1.8992
Nu_{max}	3.5280	3.5840	1.5879	3.5398	0.3345
y	0.1430	0.1375	3.8461	0.1527	6.7830
Nu_{min}	0.5860	0.5782	1.3270	0.5865	0.0853
y	1.0000	0.9875	1.2500	0.9974	0.2600

From the comparison table 4.7 it can be conclude that the obtained results are satisfactory, and that there no is much difference between the types of mesh used in this case.

Table 4.8 - DHC. Comparison results for Ra=10e5.

$Ra = 10^5$							
		Uniform 40x40 mesh		Uniform 60x60 mesh		Refined 32x32 mesh	
	Benchmark solution	Results	Error (%)	Results	Error (%)	Results	Error (%)
u_{max}	34.7300	34.7525	0.8108	34.7477	0.7969	34.6727	0.5793
y	0.8550	0.8625	0.8772	0.8583	0.3898	0.8473	0.9006
v_{max}	69.590	69.0648	0.7547	68.3620	1.7646	68.8722	1.0315
x	0.0660	0.0625	5.3030	0.0583	11.6162	0.0701	6.2121
$\overline{Nu}$	4.5190	4.8420	7.1476	4.7077	4.1757	4.4935	0.5643
Nu_{max}	7.7170	8.2092	6.3781	7.9489	3.0047	7.7566	0.5132
y	0.0810	0.0625	22.8395	0.0750	7.4074	0.0926	14.3210
Nu_{min}	0.7290	0.6778	7.02332	0.6923	5.0278	0.7251	0.5350
y	1.0000	0.9875	1.2500	0.9917	0.8333	0.9974	0.2600

In the table 4.8 is illustrated the comparison between the benchmark solution [17] and the results obtained with the code simulation. Also, it is included the results for different meshes.

Firstly, if the uniform mesh of 40x40 nodes is compared with the uniform mesh of 60x60, what is obviously to see is the results are much better when the mesh is bigger because the error decreases.

Secondly, using a refined mesh of 32x32 nodes the results are also very good, especially in the comparison of the Nusselt number. The results for Nusselt number are better using a refined mesh because this parameter is calculated at the walls and this mesh formulation have thinner control volumes near the walls.

Table 4.9 - DHC. Comparison results for Ra=10e6.

$Ra = 10^6$							
		Uniform mesh 60x60		Uniform mesh 80x80		Uniform mesh 100x100	
	Benchmark solution	Results	Error (%)	Results	Error (%)	Results	Error (%)
u_{max}	64.6300	64.9837	0.5473	64.8542	0.3469	64.7940	0.2538
y	0.8500	0.8417	0.9765	0.84375	0.7353	0.8450	0.5882
v_{max}	219.3600	220.2250	0.3943	218.908	0.2061	221.2980	0,.8835
x	0.03790	0.0417	10.0264	0.03125	17.5462	0.0350	7.6517
$\overline{Nu}$	8.8000	9.1633	4.1284	9.0203	2.5034	8.9527	1.7352
Nu_{max}	17.9250	19.6197	9.4544	18.856	10.7726	18.4189	2.7554
y	0.03780	0.0250	33.8624	0.03125	17.3280	0.0340	10.0529
Nu_{min}	0.9890	0.7039	28.8270	0.7559	24.6813	0.7897	20.1565
y	1.0000	0.9917	0.8300	0.9938	0.6250	0.9950	0.5000

The table 4.9 shows the comparison results for Ra=10^6, using three different meshes (increasing its nodes from the left to the right). As it can be seen the error decreases, at is obviously, in order that the mesh have more number of nodes. In summary, with this comparison it can be seen the results obtained for each mesh, and how the code was validated.

4.4.6. Results

Ra=10^3:

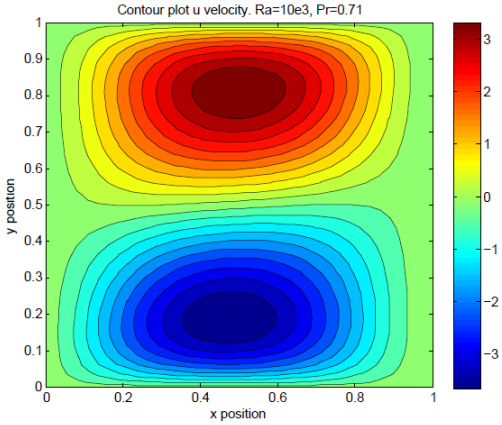

Figure 4.42 - DHC. u velocity. Ra=10e3.

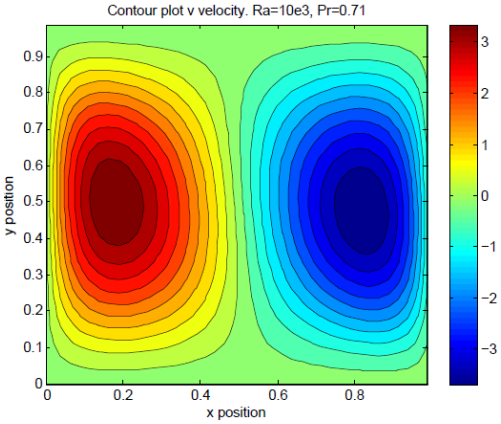

Figure 4.43 - DHC. v velocity. Ra=10e3

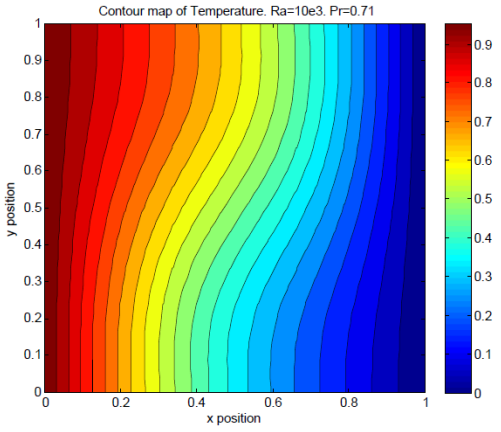

Figure 4.44 - DHC. Temperatures. Ra=10e3.

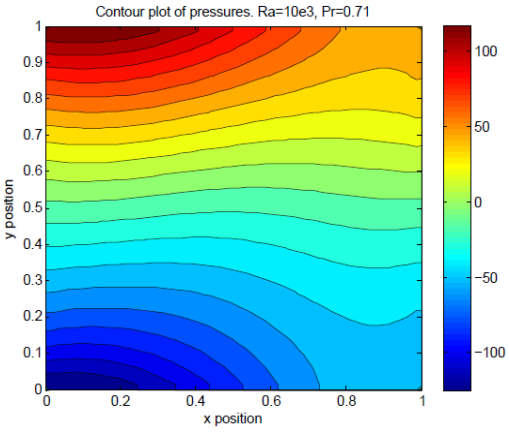

Figure 4.45 - DHC. Pressures. Ra=10e3.

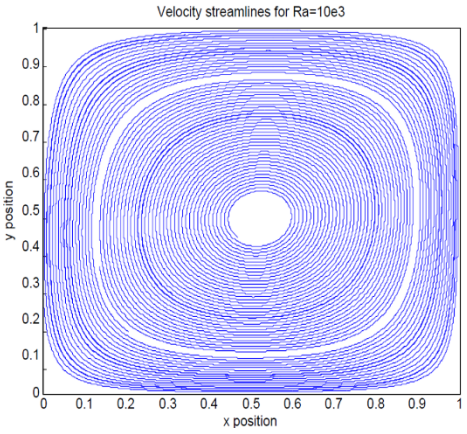

Figure 4.46 - DHC. Velocity streamlines. Ra=10e3.

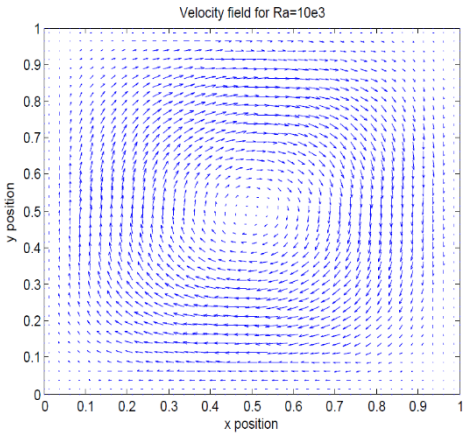

Figure 4.47 - DHC. Velocity field. Ra=10e3.

Ra=10^4:

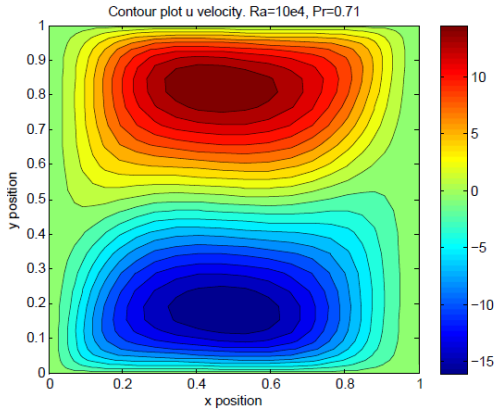

Figure 4.48 - DHC. u velocity. Ra=10e4.

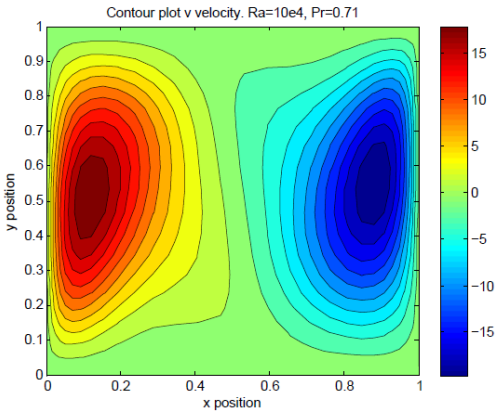

Figure 4.49 - DHC. v velocity. Ra=10e4.

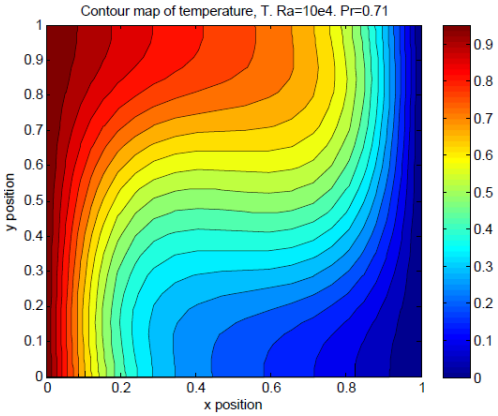

Figure 4.50 - DHC. Temperatures. Ra=10e4.

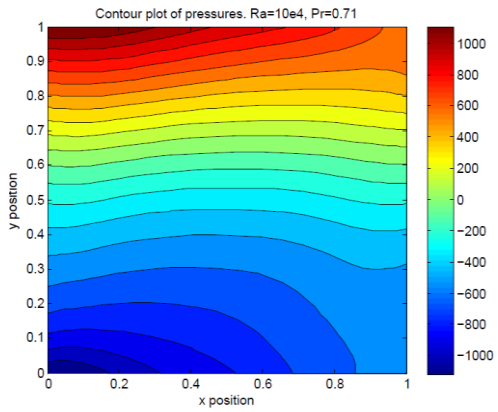

Figure 4.51 - DHC. Pressures. Ra=10e4.

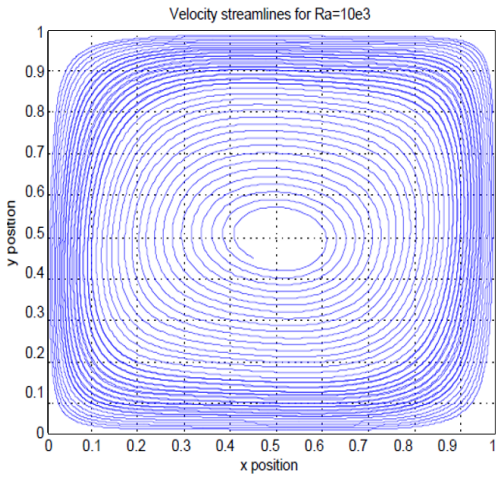

Figure 4.52 - DHC. Velocity streamlines. Ra=10e4.

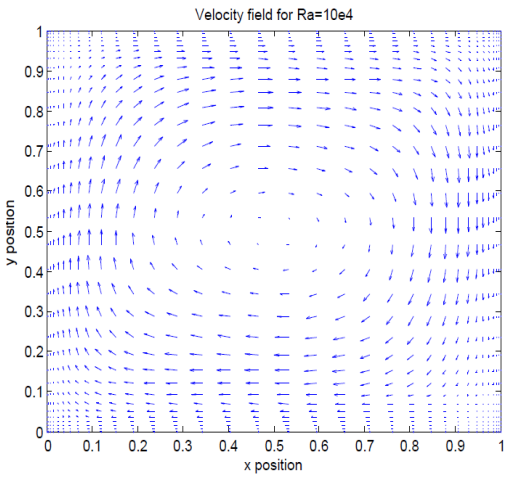

Figure 4.53 - DHC. Velocity field. Ra=10e4.

Ra=10^5:

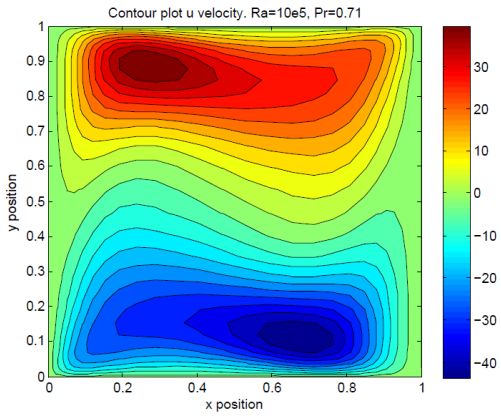

Figure 4.54 - DHC. u velocity. Ra=10e5.

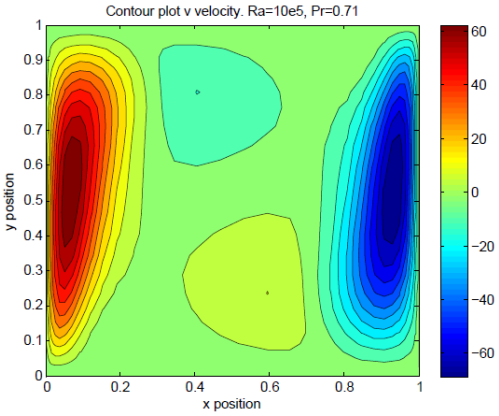

Figure 4.55 - DHC. v velocity. Ra=10e5.

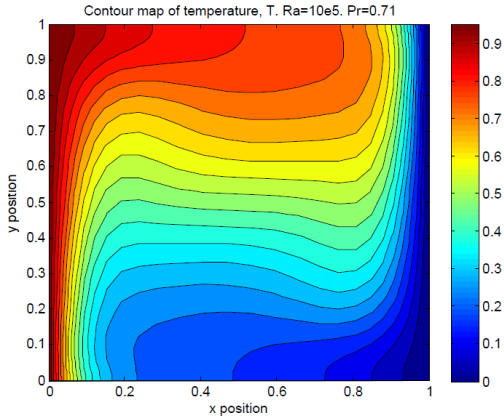

Figure 4.56 - DHC. Temperatures. Ra=10e5.

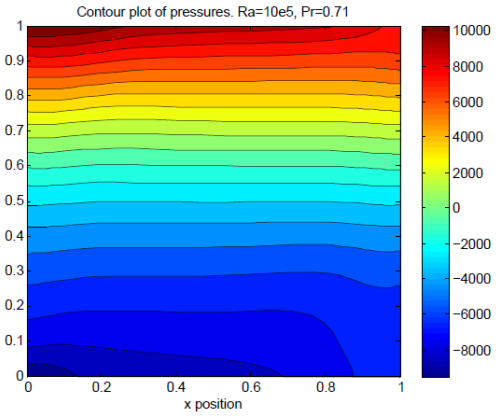

Figure 4.57 - DHC. Pressures. Ra=10e5.

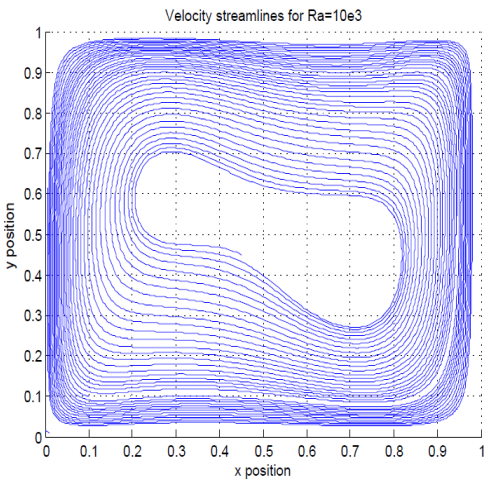

Figure 4.58 - DHC. Velocity streamlines. Ra=10e5

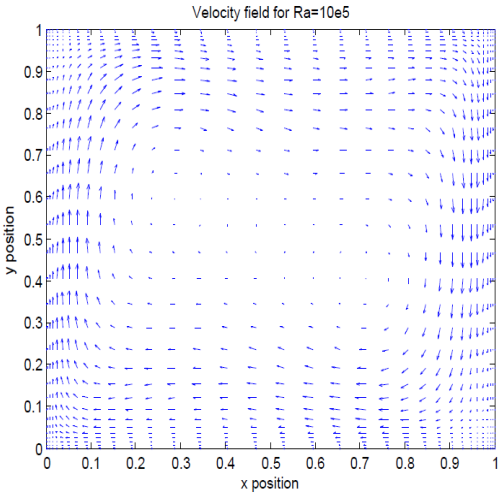

Figure 4.59 - DHC. Velocity field. Ra=10e5.

Ra=10^6:

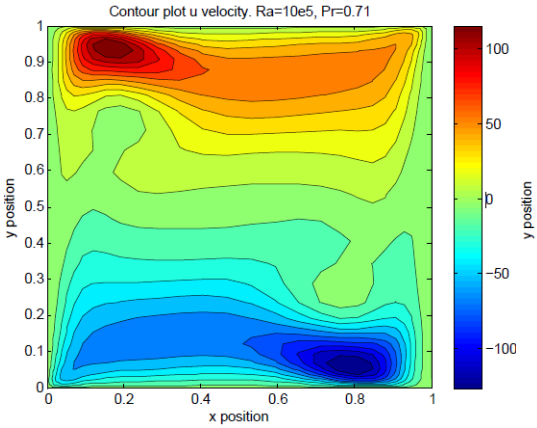

Figure 4.60 - DHC. u velocity. Ra=10e6.

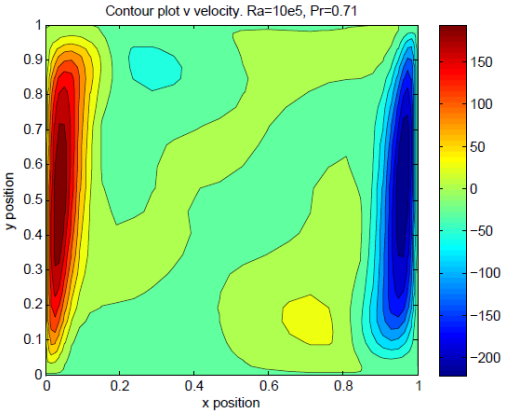

Figure 4.61 -DHC. v velocity. Ra=10e6.

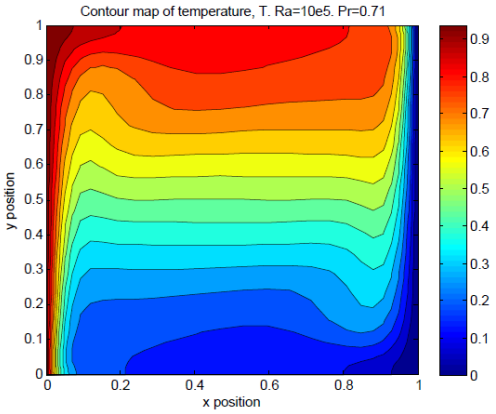

Figure 4.62 - DHC. Temperatures. Ra=10e6.

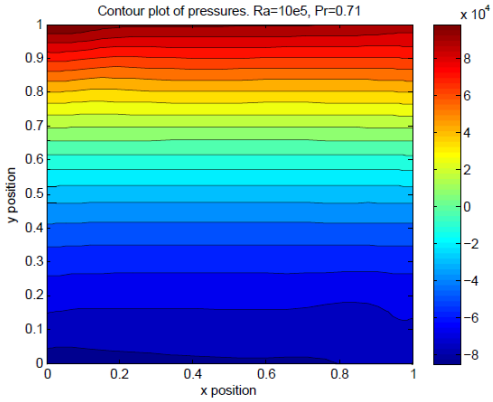

Figure 4.63 - DHC. Pressures. Ra=10e6.

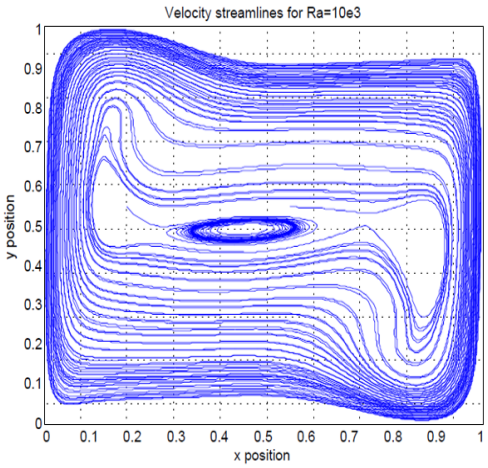

Figure 4.64 - DHC. Velocity streamlines. Ra=10e6.

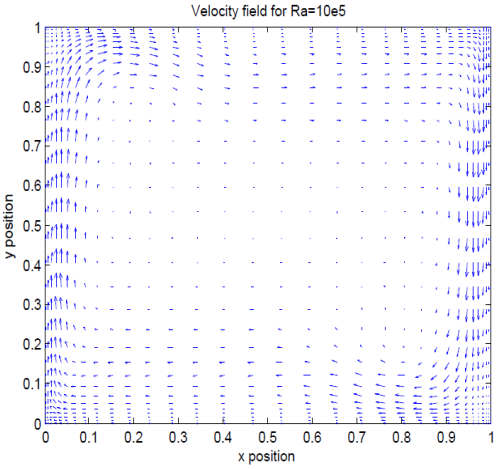

Figure 4.65 - DHC. Velocity field. Ra=10e6.

4.4.7. Analysis of the results and conclusions

The aim of this section is conclude the *differentially heated cavity* problem by analysing the obtained results while understanding all the physics involved.

The carried out simulations have been developed successfully and have been validate with making a comparison with the benchmark solution [17].

First of all, the graphs illustrated in the previous section 4.4.6 have the next objective and meaning:

- u velocity. It represents the behaviour of the dimensionless horizontal velocity component. In the red zones is where the velocity reaches its maximum value. And in the blue zones where it reaches its minimum value.
- v velocity. It represents the behaviour of the dimensionless vertical velocity component. And its zone representation is the same as the u velocity.
- Temperatures. It represents the behaviour of the dimensionless temperature inside the cavity. As it can be seen in all the cases, the left wall in red is the heated one, and the blue is the coldest.
- Pressures. It represents the behaviour of the dimensionless pressures inside the cavity, reaching its maximum in red and its minimum in blue.
- Velocity streamlines. The velocities streamlines represents the distribution of the flow inside the cavity.
- Velocity field. The velocity field representation is very similar to the velocity streamlines, with the difference that it represents the direction and the intensity of the velocity inside the cavity.

Secondly, once the previously plots are justified it is time to analyses the general behaviour of the problem and its effect in front of the variation of the Rayleigh number (the Prandtl number is not analysed because the fluid is air which means the Pr value is the same for all the simulations).

In the first place, for a Rayleigh of 10^3 the convective term does not have much effect. That can be notice because in the temperature illustration it has the form as it was a conduction problem where the fluid is heated by the left wall and that heat is transferred by the diffusive term for the rest of the cavity.

If the Rayleigh number is increased to 10^4 it may be noticed that temperature isotherms are not from a problem of just conduction, because the convective term starts having their contribution. That convective term effect also can be seen in the increases of the velocity values, which starts generating a no-perfect rotation inside the cavity.

For a Raleigh of 10^5 it can be seen how the commented aspects of Ra=10^4 increases more.

And last but not least, when the simulation is done by a Raleigh of 10^6 it clearly can be seen that the temperature transferring is commanded by the velocity movement, illustrated in the velocity streamlines figure.

And eventually, in short, this problem it has been useful to understand the resolution of the FSM when the temperature is also included.

5. APPLICATION CASE

As it has been said earlier in the introduction of the study, it will be carried out an application case of an HVAC (Heating, Ventilating and Air Conditioning) system.

In order to explain the interpretation of the problem it has been divided the explanation in some different sections. Firstly, there are introduced a few concepts of an HVAC system and also the normative associated to it. Secondly, it is made a description of the simplified problem. Thirdly, it is explained the methodology that has been carried out to solve the problem, and also the mesh that has been developed. And finally, are explained the obtained results and the conclusions drawn from them.

5.1. Introduction to HVAC

The aim of an HVAC system is to maintain a good air environment. The four variables that describes this proper environment are: the temperature, the pressure, the humidity and the ventilation. The definition and the considerations of this parameters by the regulation: *Reglamento de Instalaciones Térmicas de los Edificions, España*, are defined next.

- Temperature. The comfort zone for the temperature is between 23ºC to 25ºC in the summer, and between 21ºC to 23ºC in the winter. Those limits were defined because for example in the summer, for temperatures less than 23ºC some people may feel too cold, and for temperatures higher than 25ºC for some people may feel too warm.

- Humidity. The comfort zone for the humidity[13] is between 45% and 60% in the summer, and between 40% and 50% in the winter. Those limits values were defined because, for example, for humidity less than 45% causes that the room is too dry and that can generate effects on the health, the machines, etc. And for humidity higher than 60% the room is too muggy what would generate a mildew problem.

- Pressure. The pressure of the rooms and buildings is usually positive to reduce the outside air infiltration.

[13] These % of humidity refers to the relative humidity.

- Ventilation. The rooms have to have continuously air changes in order to get a good air quality (IAQ). And also, the air distribution has to be well done in order to keep the people of the inside comfortable without feeling any drafts.

In addition, the comfort zones may change depending of what it is contained inside the room (it is not the same having people in an office working than a room with a lot of machines).

5.2. Description of the case

The application case consists in an isothermal ventilated cavity, which intends to represent the actual ventilation of a room. To make it more as real as possible, the room has been considered as a cavity in two-dimensions, where there is an inlet slot where the cold fluid enters and an outlet slot that is for where the fluid evacuates. This representation is showed in the next figure 5.1.

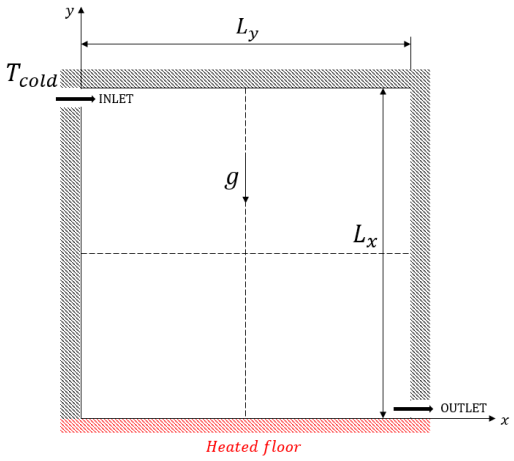

Figure 5.1 - Schema of the application case.

This case was experimental solve by Balay and Mergui [18]. And it has been also consulted the paper [19] as a reference problem.

In the beginning, the cavity has no velocity and the map of temperatures is all constant at 32ºC. Then, it starts entering cold fluid from the inlet slot, and at the same time it is evacuated cold fluid for the outlet slot. Therefore, the aim of this problem is be able to simulate how the cavity is cooled, by solving the NS equations using the FSM.

5.2.1. Physical characteristics and geometry

Physical characteristics:

- The cold air that enters on the inside of the cavity, $T_c = 15℃$
- The heat air that is initially on the inside of the cavity, it is a temperature$T_h = 32℃$. Moreover, the heated floor of the room it is also at T_h temperature.
- The velocity that enters from the inlet slot, is determined by a parabolic profile with maximum velocity $U_{in} = 0.65\ m/s$.

The needed air properties are defined in the table 5.1.

Table 5.1 - Air physical characteristics

Pr	k_{air}	ν_{air}
0.71	2.1×10^{-5}	1.5×10^{-5}

Geometric characteristics:

- The height and the width of the cavity are both $Lx = Ly = 1.04m$.
- The inlet slot has a height of $h = 0.05m$.
- The outlet slot has a height of $l = 0.05m$.

5.2.2. Boundary conditions

In order to be able to solve this problem it is needed to define the boundaries conditions for the two components of the velocity and also for the temperature. The boundary conditions are defined in the following point:

- The temperatures. For all the adiabatic walls, the BC is $\frac{\partial T}{\partial n} = 0$. For the bottom wall the temperature is isothermal fixed in $T = T_h$. For the inlet slot the temperature is isothermal fixed in $T = T_h$, and for outlet slots the Neumann condition ($\frac{\partial T}{\partial n} = 0$).

- The vertical component of the velocity. This is the easiest BC because the velocity is at all the walls fixed to zero.

- The horizontal component of the velocity. In all the walls is fixed to zero, except in the inlet and outlet slots.

For the inlet slot the velocity is imposed by the parabolic velocity profile, as it is shown in the figure 5.2.

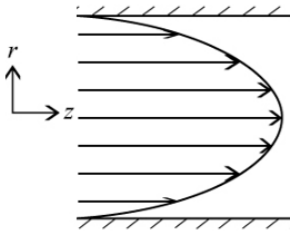

Figure 5.2 - HVAC case. Inlet boundary condition.

In the next equation it is described the formula to find the velocity at each point of the inlet slot:

$$u(r) = U_{max}\left(1 - \frac{r^2}{R^2}\right) \tag{5.1}$$

Where U_{max} is the maximum velocity. R is the distance between the wall and the centre of the parabolic profile. And r is the distance from the centre to the point where the velocity is wanted to be calculated.

And at the outlet slot it is needed to consider that $\frac{\partial u}{\partial n} = 0$.

5.3. Mathematical formulation

As the problem consists in a mixed convection, it is needed to be solved using the NS in the dimensionless variables of mixed convection[14].

These equations are defined next:

$$\frac{\partial \hat{u}}{\partial \hat{x}} + \frac{\partial \hat{v}}{\partial \hat{y}} = 0 \tag{5.2}$$

$$\frac{\partial \hat{u}}{\partial \hat{t}} + \hat{u}\frac{\partial \hat{u}}{\partial \hat{x}} + \hat{v}\frac{\partial \hat{u}}{\partial \hat{y}} = -\frac{\partial \hat{p}}{\partial \hat{x}} + \frac{1}{Re}\left(\frac{\partial^2 \hat{u}}{\partial \hat{x}^2} + \frac{\partial^2 \hat{u}}{\partial \hat{y}^2}\right) \tag{5.3}$$

$$\frac{\partial \hat{v}}{\partial \hat{t}} + \hat{u}\frac{\partial \hat{v}}{\partial \hat{x}} + \hat{v}\frac{\partial \hat{v}}{\partial \hat{y}} = -\frac{\partial \hat{p}}{\partial \hat{y}} + \frac{1}{Re}\left(\frac{\partial^2 \hat{v}}{\partial \hat{x}^2} + \frac{\partial^2 \hat{v}}{\partial \hat{y}^2}\right) + \frac{Ra \cdot \theta}{Re \cdot Pe} \tag{5.4}$$

$$\frac{\partial \theta}{\partial \hat{t}} + \hat{u}\frac{\partial \theta}{\partial \hat{x}} + \hat{v}\frac{\partial \theta}{\partial \hat{y}} = \frac{1}{Re \cdot Pe}\left(\frac{\partial^2 \theta}{\partial \hat{x}^2} + \frac{\partial^2 \theta}{\partial \hat{y}^2}\right) \tag{5.5}$$

Where the values of $\hat{u}$ and $\hat{v}$ are the dimensionless velocities. $\hat{t}$ is the dimensionless time. The components $\hat{x}$ and $\hat{y}$ are the dimensionless of x and y, respectively. $\hat{p}$ is the dimensionless variable of the pressure. And finally, the variable θ defines the dimensionless temperature.

[14] Please refer to Annex A.3 to see the deduction of the non-dimensionalization of the NS equations in mixed convection.

Moreover, the dimensionless numbers that appeared in the equations from 5.2 to 5.5, are defined next.

$$Re = \frac{U_{in} Lx}{\nu} \tag{5.6}$$

$$Pr = \frac{\nu}{k} \tag{5.7}$$

$$Ra = \frac{\beta g L^3 \Delta T}{\nu\, k} \tag{5.8}$$

Moreover, apart from these dimensionless numbers, for this problem it is very useful to pay attention to the values of the Archimedes and Froude numbers:

$$Ar = \frac{g\beta h \Delta T}{{U_{in}}^2} \tag{5.9}$$

$$Fr = Ar^{-1/2} = \frac{U_{in}}{\sqrt{g\beta h \Delta T}} \tag{5.10}$$

The Archimedes number Ar, shown in the equation 5.9, is the ratio of gravitational force to viscous force. And the Froude number, indicated in the equation 5.10, is the dimensionless quantity used to indicate the influence of graviton fluid mention.

Finally, to solve these equations, the procedure is the same as it has been defined in the earlier problems. The only difference is in the evaluation of the diffusive and the convective terms where the expressions will have the mixed convection dimensionless numbers as in the equations from 5.2 to 5.5.

5.4. Mesh

The used mesh is showed in the next figure 5.3. As the figure represents, the mesh is thinner in the top and bottom walls. The justification of this formulation is because inlet and outlet slots are very small. Therefore, it could appear some resolution problems if the mesh is not thin enough in those zones.

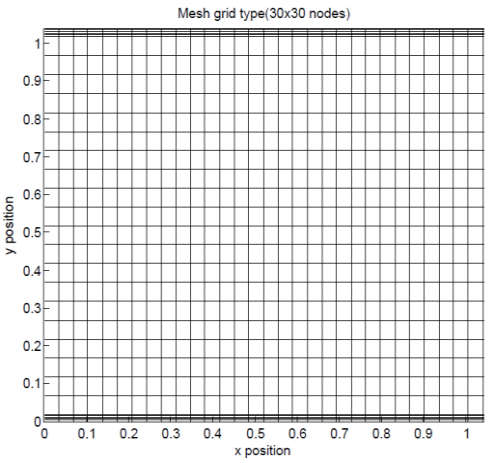

Figure 5.3 - HVAC case mesh, using 30x30 nodes.

5.5. Analysis of the results

In this section are represented and commented the results that have been obtained with the simulation of this application case. The explanation of the results is divided in two sections: the velocities and the temperatures, which are the important variables to focus on, due to they will de determine the ventilation of the room.

Nonetheless, please refer to the Annex D.1 for further information of the results of this HVAC case. However, in the Annex D.2 it can be found a variation from the basic problem in order to understand better the ventilation of the room, and the importance of the dimensionless numbers that define the resolution of this problem.

5.5.1. Velocity

In the next figure 5.4, it can be seen the how the fluid movement into the cavity.

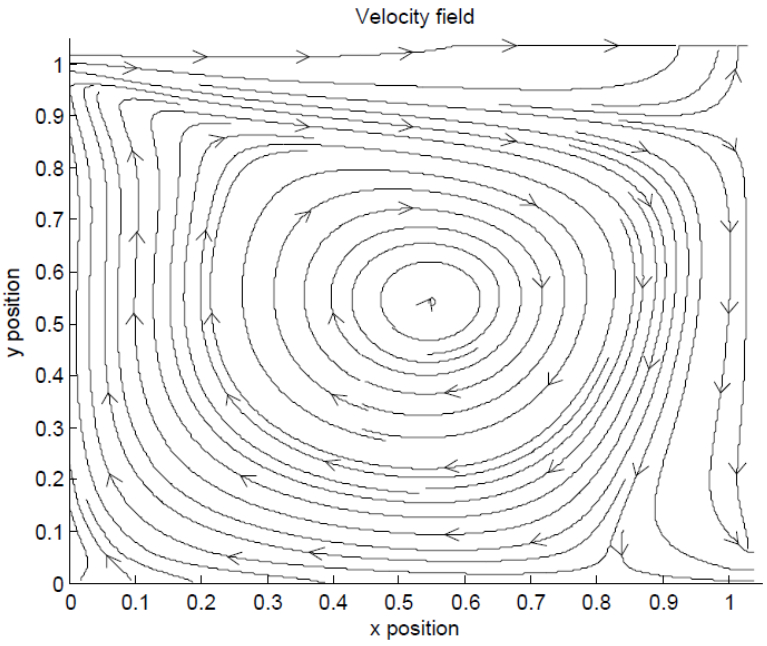

Figure 5.4 – HVAC case. Velocity field.

As the figure shows, the fluid gets inside of the cavity for the left top of the cavity, and it moves making a clockwise rotation, and finally gets out of by the outlet slot, which is situated in the bottom left wall.

5.5.2. Temperatures

As the objective of the problem raised is to solve the ventilation inside of a cavity, it is very interesting to see how the temperature evolves during the time. That transient behaviour is showed below.

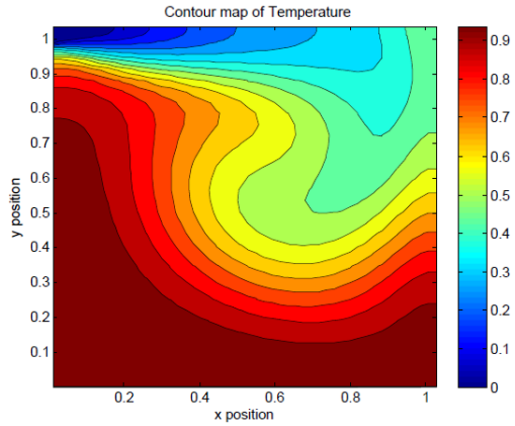

Figure 5.5 - HVAC case. Temperature map at t=20s.

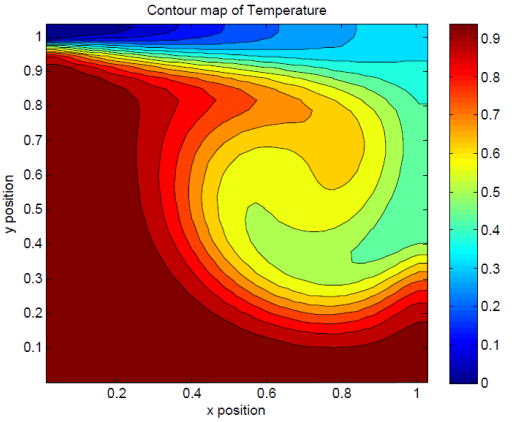

Figure 5.6 HVAC case. Temperature map at t=40s.

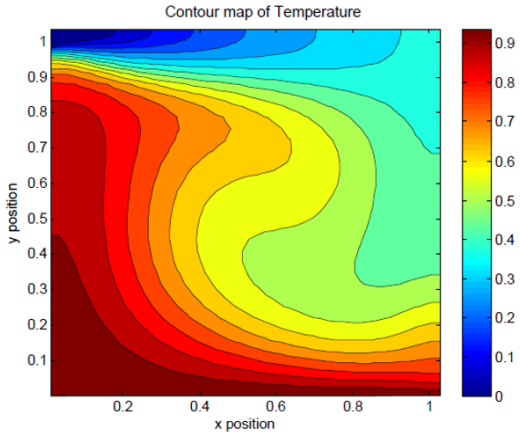

Figure 5.7 - HVAC case. Temperature map at t=60s.

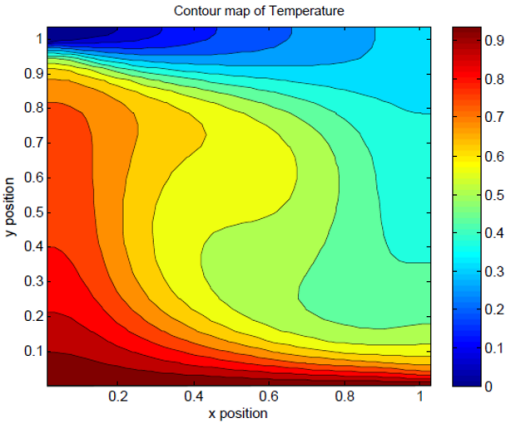

Figure 5.8 - HVAC case. Temperature map at t=100s.

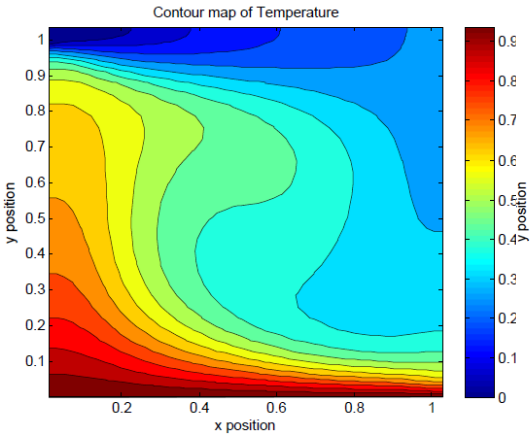

Figure 5.9 - HVAC case. Temperature map at t=250s.

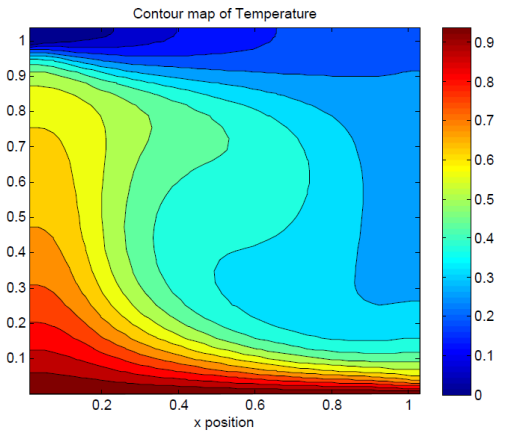

Figure 5.10 - HVAC case. Temperature map at almost t=400s.

The previous figures, from 5.5 to 5.10, is shown the cooling evolution during the time inside the cavity. In the first figure 5.5, it can be clearly seen how the cooler fluid gets inside of the cavity from the inlet slot. And following its next figures it can be appreciated how the strong red zone is being removed by the green and blue colours, which means a lower temperatures.

Moreover, in all the figures it can be seen that the left part of the cavity is always the hottest and the right one the coolest. That is due to the clockwise rotation moving of the fluid that has been created at the inside of the cavity.

Furthermore, if it is wanted to analyse the real temperature behaviour, that is to say work with the real temperature. For example, in the figure 5.9 the major part it is at temperature of 0.4 (light blue). Those values of temperature are in its dimensionless variable, so the real temperature of this light blue zone will be: $T = 0.4 \cdot (32 - 15)℃ + 15\ ℃ = 21.80\ ℃$. Which means that the comfort winter zone is reached, due to the temperature is between 21 and 23ºC.

5.5.3. Conclusions of the application case

With the aim of making a general conclusion of application case that has been solved, it has to be said that it was very useful to get familiar with the resolution of CFD applied in a HVAC problem.

Firstly, it has been solved the basic problem as it was defined in the description of the case, ant it has been analysed the cavity behaviour for the velocities and the temperatures in order to understand how it works.

Secondly, with the purpose of making a more exhaustive study of the problem, some modifications and variations has been introduced and analysed. And understanding how the fluid behaviour changed.

And finally, as a general summary, it has been learned how to be critic in front of a HVAC graph with making its interpretation and check if the solution it can be physically possible of if not. Moreover, by using the current HVAC Spanish regulation, the results have been analysed to determine if at each different configuration the solution satisfies the regulation temperature limits.

6. ECONOMIC AND ENVIROMENTAL STUDY IMPACT

In this section, the environmental and economic implications of the study are appraises, in order to determinate its viability.

6.1. Economic impact analysis

To see the calculation of the calculation of the total cost of this study please refer to the budged document. Even so, the next table summarizes the final results, which have been considered viable.

Table 6.1 - Total cost of the study.

ELEMENT	COST [€]	
Human resources	7600.00	
Hardware	59.93	
Software	97.00	
	TOTAL COST	**7756.93 €**

6.2. Environmental impact assessment

The only aspect of this study that could have an environmental impact is the laptop energy consumption. Because in this study it has not been used nothing more than a laptop and a few sheets of paper (which are not included in this environmental study because its impact will be virtually zero).

In order to find the ecological footprint emitted in the developing of this project. First it would be needed to know the power consumption of the used laptop.

The power consumption of a laptop can be found looking AC adapter. For the used one, the voltage and the intensity are 240V and 1.5A, respectively. Therefore, the consumption is: $240V \cdot 1.5A = 360W = 0.36kW$.

Once the consumed watts of the machine are known, we transform those W in the units of CO_2 emitted by multiplying the worked hours[15] with the emissions[16] ($gr\ CO_2/kWh$) and finally multiplied with the power consumption calculated.

[15] The worked ours are determined by the multiplication of the worked weeks, the number of days worked per week and the hours for each day. Which are $: 16\,weeks \cdot 5\,days/week \cdot 4\,hours/week = 320\,h$

[16] The $gr\ CO_2/kWh$ emitted can be found in the reference [20].

This calculations are showed next.

$$0.36kW \cdot 320h \cdot 649\ gr\frac{CO_2}{kWh} = 74764.8\ grCO_2 = \mathbf{74.765\ kg\ CO_2}$$

With those values of CO_2 emissions it can be clearly considered that this study does not create a huge negative impact. The reason is clear: This is a study that has been carried out using a normal laptop to do simulations.

However, it is important to mention that one of the objectives of this project is to get familiar with the engineering fluid mechanics tools that are used in real applications, such it can be the machines design or the pattern of more efficient thermic systems, and therefore, reducing its environmental impact.

Furthermore, it is also important to underline that in the real engineering application cases, the CFD simulations consumption is much lower than what it would be consumed if the same problem was solved by experiment, which will be the wind tunnel. What is more, making a comparison between the wind tunnel and the CFD simulation, it is easy to see how the simulation has lower environmental impact. The only thing in the using of simulation that can create impact is the energy consumption, which can be higher in the case of solving a very huge problem for which it is needed the use of a supercomputer. However, using the wind tunnel, apart from the energy consumption, there is all the things that form the wind tunnel, what makes its impact increases more and more.

Therefore, it is more viable the use of the computer simulation in front of the experimentation, in order to reduce the environmental impact.

7. PLANNING AND SCHEDULING OF THE STUDY

In this section are defined the tasks that have been carried out in the development of this study.

7.1. Identification and description of the study tasks

Table 7.1 - Planning tasks of this study.

COD	Activity	Description
1.1	Project start	
2.1	Background study	Understand and identify the importance of solving the conservation equations of mass, energy and momentum applied in engineering problems.
3.1	Theory learning of numerical methods for CFD	Review the theory knowledge about numerical methods to be applied in the resolution of heat transfer and fluid dynamics problems. Study the different methods and models.
3.2	Solve a two - dimensional transient conduction problem	Implementation of a C++ code to solve a two-dimensional conduction problem, and optimize this code.
3.3	Solve a two-dimensional steady convection-diffusion equation problem	Implementation of a C++ code to solve a two-dimensional problem where conduction and diffusion are involved, while using the resolution of convection-diffusion equation. Additionally, optimize the code.
3.4	Solve the *Driven-Cavity* problem	Implementation of a C++ code to solve a two-dimensional forced convection problem using the Fractional Step Method to solve the Navier-Stokes equations. Additionally, optimize the code.
3.5	Solve the *Differentially Heated Cavity* problem	Adapt the *Driven Cavity* problem in order to solve the *Differentially Heated Cavity*, adding and changing the equations in order to solve the natural convection in a cavity. Additionally, optimize the code.
4.1	Propose the particular case	Define the variables involved in the particular case, its geometry and characteristics.

4.2	Implement the particular case	Development of the C++ code for the purpose of solve the particular case.
4.3	Verification of the code	Checking that the code works well.
4.4	Validation of the code	In order to validate the code, different solved cases will be compared and checked.
4.5	Particular case optimization	Modify the code in order to validate the particular case. Optimization of the mesh.
4.6.	Getting the finale results of the particular case	Get the results through the implemented code. Failing that, it will be made a planning about how this project could be finish and extended to develop a master's degree final project.
5.1	Finale conclusions	Make the final conclusions of the study, based in the obtained results from the particular case.

To see the Gantt chart of those tasks, please refer to section 7.2.

7.2. Gantt chart of the study

Id	COD	Nombre de tarea	Duración	Comienzo	Fin	Predecesoras
1	1	**Final degree project**	**89 días**	**lun 09/02/15**	**vie 12/06/15**	
2	1.1	Project start	0 días	lun 09/02/15	lun 09/02/15	
3	2.1	Background study	2 días	lun 09/02/15	mar 10/02/15	2
4	3.1	Theory learning of numerical methods for CFD	5 días	vie 13/02/15	jue 19/02/15	3
5	3.2	Solve a two-dimensional transient conduction problem	5 días	vie 20/02/15	jue 26/02/15	4
6	3.3	Solve a two-dimensional steady convection-diffusion equation	6 días	vie 27/02/15	vie 06/03/15	5
7	3.4	Solve the Driven-Cavity problem	9 días	lun 09/03/15	jue 19/03/15	6
8	3.5	Solve the Differentially Heated Cavity problem	6 días	vie 20/03/15	vie 27/03/15	7
9	4.1	Proposte the particular case	2 días	lun 30/03/15	mar 31/03/15	8
10	4.2	Implement the code of the particular case	19 días	mié 01/04/15	lun 27/04/15	9
11	4.3	Verification of the code	2 días	mar 28/04/15	mié 29/04/15	10
12	4.4	Validation of the code	2 días	jue 30/04/15	vie 01/05/15	11
13	4.5	Particular case optimization	5 días	lun 04/05/15	vie 08/05/15	12
14	4.6	Getting the finale results of the particular case	7 días	lun 11/05/15	mar 19/05/15	13
15	5.1	Finale conclusions	7 días	jue 21/05/15	vie 29/05/15	14
16	-	Project Charter	0 días	vie 06/03/15	vie 06/03/15	
17	-	Follow up, one	0 días	vie 20/03/15	vie 20/03/15	
18	-	Follow up, two	0 días	vie 10/04/15	vie 10/04/15	
19	-	Follow up, three	0 días	vie 01/05/15	vie 01/05/15	
20	-	Preliminary delivery	0 días	vie 29/05/15	vie 29/05/15	15
21	-	Final delivery	0 días	vie 12/06/15	vie 12/06/15	

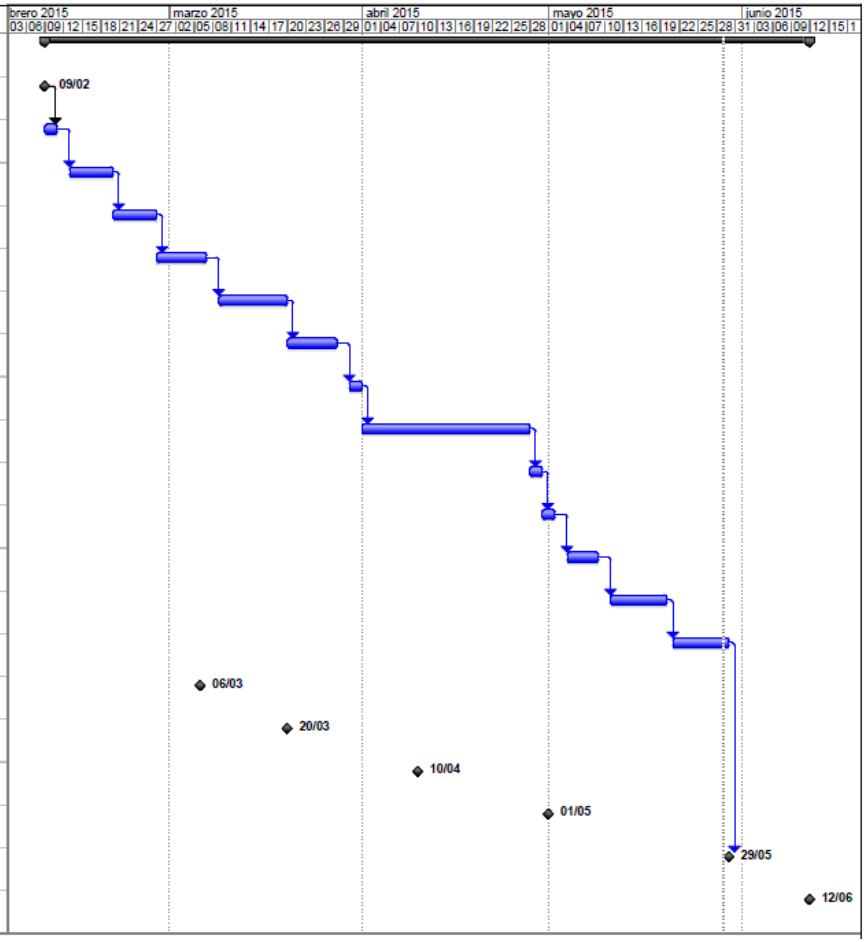

8. FUTURE PLANNING AND SCHEDULING

In this section are defined the tasks that could be carried out in a future final degree project or a final master's degree.

8.1. Identification and description of the future tasks

Table 8.1 - Planning tasks for the future development of the continuation of this study.

COD	Activity	Description
1.1	Project start	
2.1	Introduction to turbulence	Understand the physics and the differences between the turbulence and the laminar regime. And learn all the involved theory in the resolution of turbulence cases.
2.2	Solve the Burges equation problem	Implement a C++ code that solve the Burges equation. Check different "meshes" to analyse its results.
2.3	Solve the Burges equation problem using the LES models	Modify the previous Burges equation code to introduce the using of LES models and analyse its results.
3.1	Solve the numerical simulation of turbulent flow in the differentially heated cavity in 2D.	From the differentially heated code implemented, adapt that code to solve the same problem but now with an aspect ratio 4 (the width is four times smaller than the height). Analyse its turbulent behaviour. Check and analyse its results.
3.4	Solve the numerical simulation of turbulent flow in the differentially heated cavity in 3D.	Solve the same problem as in 3.1, but extending it to the third dimension, adding all the new parameters that have to be considered in a three dimension problem. Its results will be checked and analysed.
3.5	Solve the turbulent mixed convection in a 3D ventilated cavity	By using the LES models, solve the turbulent mixed convection in a ventilated cavity, in all the three dimensions. Check and analyse its results.

4.1	Propose a particular case of turbulence to solve	Search a turbulent problem that could have an engineering real application. Define its characteristics, geometry and physics involved.
4.2	Implement the particular case	Develop a C++ code for the purpose particular case to solve.
4.3	Verification of the code of the case	Check that the develop code works well, and that it does not have any compilation problem.
4.4.	Validation of the code of the case	Validate the obtained results.
4.5	Particular case optimization	Modify the code in order to correctly understand the fluid behaviour on the defined geometry and domain.
4.6	Getting the finale results of the particular case	Get the final results through the implemented code, and analyse them in detail.
5.1	Finale conclusions	Make the final conclusions of the study, based in the obtained results of the developed problems.

To see the Gantt chart of the possible future study please refer to section 8.2.

8.2. Future Gantt chart

	COD	Nombre de tarea	Duración	Comienzo	Fin	Predecesoras
1	**1**	**Final degree project**	**88 días?**	**lun 01/06/15**	**mié 30/09/15**	
2	1.1	Project start	0 días	lun 01/06/15	lun 01/06/15	
3	2.1	Introduction to turbulence	7 días	lun 01/06/15	mar 09/06/15	2
4	2.2.	Solve the Burges equation problem	3 días?	mié 10/06/15	vie 12/06/15	3
5	2.3.	Solve the Burges equation problem using the LES models	3 días	lun 15/06/15	mié 17/06/15	4
6	3.1	Solve the numerical simulation of turbulent flow in a differentially heated cavity in 2D	5 días	vie 26/06/15	jue 02/07/15	5
7	3.2	Solve the numerical simulation of turbulent flow in a differentially heated cavity in 3D	11 días	vie 03/07/15	vie 17/07/15	6
8	3.3	Solve the turbulent mixted convection in a 3D ventilated cavity	7 días	lun 20/07/15	mar 28/07/15	7
9	4.1	Proposte the particular case of turbulence to solve	3 días	vie 31/07/15	mar 04/08/15	8
10	4.2	Implement the code of the particular case	13 días	mié 05/08/15	vie 21/08/15	9
11	4.3	Verification of the code of the case	5 días	lun 24/08/15	vie 28/08/15	10
12	4.4	Validation of the code of the case	4 días	jue 03/09/15	mar 08/09/15	11
13	4.5	Particular case optimization	6 días	mié 09/09/15	mié 16/09/15	12
14	4.6	Getting the finale results of the particular case	7 días	jue 17/09/15	vie 25/09/15	13
15	5.1	Finale conclusions	3 días	lun 28/09/15	mié 30/09/15	14
16	-	Final delivery	0 días	mié 30/09/15	mié 30/09/15	15

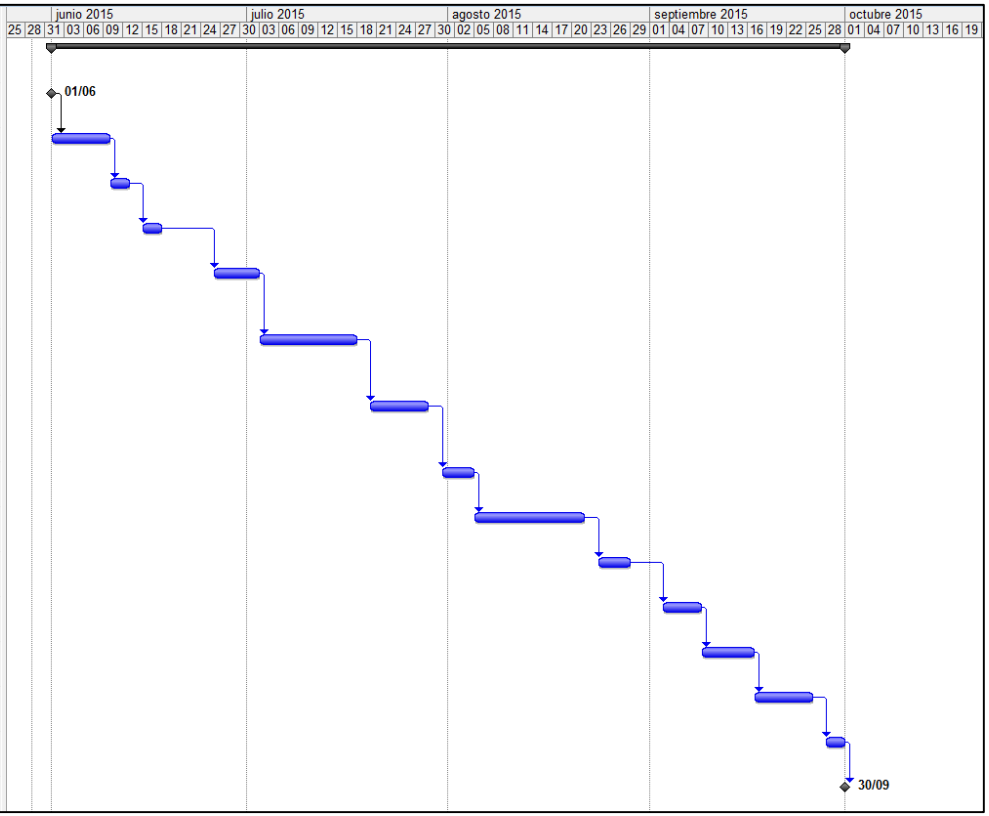

9. FUTURE LINES

The next steps that could be carried out after this study could be continuing working in the code implementation on particular cases, with the aim of keeping advancing in the consolidation of the numerical methods applied to the solving of Navier-Stokes equations.

In this study it has only been performed the resolution of the NS equations in the laminar regime. Therefore, the next step should be the introduction of the turbulence and solve some several cases of it.

In a beginning, turbulence cases should be only in two dimensions. After that, in order to move a high step, the turbulent problems could be in three dimensions (that is how the turbulence problems has to be properly treated). To start treating turbulence problems it will have to be introduced the LES models (Large Eddy Simulations). What those models make is use a velocity "filter" in order to eliminate the small scales of solution, because in turbulence working with small scales does not give an accurate solution. But, solving a turbulence problem using the DNS (Direct Numerical Simulation) is too expensive because the needed meshes are very big and the computing-time and the energy needed is too much. So, LES models, give us a way to reduce the cost of a project and also get a good solution.

In conclusion, in order to continue learning about the numerical resolution of the Navier-Stokes equations in the turbulent regime, it will be implemented from more easy to more difficult, some different turbulent problems.

10. CONCLUSIONS

In the introduction of the study, it has been said that the aim was to be able to develop a CFD&HT capable to solve the Navier-Stokes equations.

To do so, firstly it was needed to learn and understand the theoretical background, where were explained the physics and the numerical methodology to solve those equations.

Secondly, the theoretical knowledge learned has been applied in solving four particular cases in order from least to most difficult:

- The resolution of the conduction problem of a beam made of four different materials.
- The introduction to the convection by solving a two dimensional convection problem where the velocity field is known.
- The properly resolution of the Navier-Stokes equations in a forced convection case in a squared cavity.
- And finally, the adaption of the resolution of the NS equations in a natural convection case, which means that in addition the temperature needs to be solved.

Furthermore, those problems have been useful to check its solution with its benchmark in order to verify its implementation.

Thirdly, once the basics problems were solved the next step was to specifically resolve an engineering real case, which was a simplified HVAC (Heating, Ventilating and Air Conditioning) case. With which it has been learned, apart from its physical and numerical implementation, to be able to analyse and be critic front the results.

In general summary, this study has been very useful to understand and develop some practical CFD&HT transfer problems, and also solve a particular case that, as far I am concern, it is a very interesting application of engineering.

11. REFERENCES AND REGULATIONS

11.1. References

[1] "Merriam-Webster. An Encyclopedia Britannica Company," 11 May 2015. [Online]. Available: http://www.merriam-webster.com/dictionary/hvac.

[2] National Aeronautics and Space Administration (NASA), "Navier-Stokes Equations," [Online]. Available: https://www.grc.nasa.gov/WWW/k-12/airplane/nseqs.html. [Accessed 20 May 2015].

[3] National Aeronautics and Space Administration (NASA), "Euler Equations," Glenn research center, [Online]. Available: https://www.grc.nasa.gov/www/K-12/airplane/eulereqs.html. [Accessed 20 May 2015].

[4] A. Thom, "The Flow Past Circular Cylinders at Low Speeds," *Proc. Royal Society,* vol. 141, no. 845, pp. 651-666, 1933.

[5] M. Kawaguti, "Numerical Solution of the NS Equations for the Flow Around a Circular Cylinder at Reynolds Numer 40," *Journal of Physics society, Japan,* vol. 8, pp. 747-757, 1953.

[6] S. V. Patankar, Numerical Heat Transfer and FLuid FLow, Hemisphere Publishing Corporation, 1980.

[7] J. H. Ferziger and M. Peric, Computational Methods for Fluid Dynamics, New York: Springer-Verlag, 2002.

[8] F. Harlow and E. Welch, "Numerical calculation of time-dependent viscous incompressible flow of fluid with free surface," *Physics of Fluids,* no. 8, p. 21822189, 1965.

[9] A.-. J. Chorin, "Numerical solution of the Navier-Stokes equations," *Mathematics of Computation,* no. 22, pp. 746-762, 1968.

[10] Centre Teconològic de Transferència de Calor, Terrassa, Espanya. , "Introduction to the Fractional Step Method.," Universitat Politècnica de Catalunya, Terrassa, Espanya, 2013.

[11] Courant, R., Friedrichs, K. and Lewy, H. , "Über die partiellen Differenzengleichungen der mathematischen Physik," *Mathematische Annalen, 100,* pp. pp. 32-74, 1928.

[12] E. Simons, "An efficient muti-domain approach to large eddy simulation of incompressible turbulent flows in complex geometries.," in *PhD thesis, Von Karman Institute for Fluid Dynamics*, October 2000.

[13] Smith, R. M. and Hutton, A. G., "The numerical treatment of advection: a performance comparison of current methods.," in *Numerical Heat Transfer, 5*, 1982, pp. pp 439-461.

[14] Ghia, U., Ghia, K.N., and Shin, C.T., "High-Re Solutions for Incompressible Flow Using the Navier-Stokes Equations and Multigrid Method," *Journal of Computational Physics,* pp. pp 387-411, 1982.

[15] Auteri, F., Parolini, N. and Quartapelle, L., "Numerical investigation on the stability of singular driven cavity flow.," *Journal of Computational Physics, Vol 183, (1).,* pp. pp 1-25, 2002.

[16] Bruneau, C-H. and Saad, M., "The 2D lid-driven cavity problem revisited," *Computers & Fluids 35,* pp. pp. 326-348, 2006.

[17] De Vahl Davis, G., "Natural convection of air in a square cavity a benchmark numerical solution," *International Journal for Numerical Methods in Fluids,* vol. 3, pp. Vol. 3, pp 249-264, 1983.

[18] D. Balay, S. Mergui, J. L. Tuhault and F. Penot, "Eperimental turbulent mixted convection created by confined buoyant wall jets.," *First Eur Heat Transfer Conf, UK,* pp. 821-828, 2992.

[19] R. Ezzouhri, P. Joubert, F. Penot and S. Mergui, "Large Eddy simulation of turbulent mixed convection in a 3D ventilated cavity: Comparison with existing data.," *International Journal of Thermal Sciences,* no. 48, 2009.

[20] McDonough, J. M., Introductory lectures on turbulence, University of Kentucky: Deparments of Mechanical Engineering and Mathematics , 2007.

[21] De Vahl Davis, G. , "Natural convection of air in a square cavity a comparison exercise," *International Journal for Numerical Methods in Fluids,* vol. 3, pp. Vol. 3, pp 227-248, 1983.

[22] "Secretaría de estado de energía.," Ministerio de Industria, Energía y Turismo, Gobierno de España. , 3 3 2014. [Online]. Available: http://www.minetur.gob.es/energia/desarrollo/EficienciaEnergetica/RITE/Paginas/InstalacionesTermicas.aspx. [Accessed 22 5 2015].

[23] W. Malalasekera and H. K. Versteeg, An introduction to computational fluid dynamics. The finite volume method, Harlow, England: Longman House, 1995.

[24] "Fluid Mechanics," Wikipedia, 7 January 2015. [Online]. Available: http://simple.wikipedia.org/wiki/Fluid_mechanics. [Accessed 20 May 2015].

[25] "Introduction to the Fractional Step Method," *CTTC, Centre Tecnològic de Transferència de Calor, Terrassa, Espanya,* 2013.

[26] D. Kuzmin, Introduction to Computational Fluid Dynamics., University of Dortmund, p. 5: Institute of Applied Mathematics.

[27] "Numerical methods", CFD Online. Available: http://www.cfd-online.com/Wiki/Numerical_methods. [Accessed 9 April 2015].

[28] "Graphis", MatlhWorks. Available: http://es.mathworks.com/help/matlab/graphics.html [Accessed 13 April 2015]

11.2. Regulations

[1] Reglamento de Instalaciones Térmicas de los Edificios. Aprobado por el Real Decreto 1027/207, el 20 de julio de 2007.